DEVELOPMENT OF EFFECTIVE NUMERICAL SCHEMES FOR FRICTIONAL HEAT GENERATION AND DIFFUSION IN VIBROTHERMOGRAPHY

by

Darren Joseph Platt

A thesis submitted in partial fulfillment
of the requirements for the degree

of

Master of Science

in

Mechanical Engineering

MONTANA STATE UNIVERSITY
Bozeman, Montana

November, 2012

APPROVAL

of a thesis submitted by

Darren Joseph Platt

This thesis has been read by each member of the thesis committee and has been found to be satisfactory regarding content, English usage, format, citations, bibliographic style, and consistency, and is ready for submission to The Graduate School.

Dr. Ahsan Mian

Approved for the Department of Mechanical and Industrial Engineering

Dr. Chris Jenkins

Approved for The Graduate School

Dr. Ronald W. Larsen

STATEMENT OF PERMISSION TO USE

Darren Joseph Platt

November, 2012

ACKNOWLEDGEMENTS

I would like to thank my advisors, Dr. Mian and Dr. Cairns, for their help on this thesis. I also express my gratitude to Corey Cook, with whom this has been a collaboritive process. The other poeple I would like to thank are Peter Lucon and Resodyn Corporation for their guidance and funding, respectively.

TABLE OF CONTENTS

TABLE OF CONTENTS – CONTINUED

LIST OF TABLES

Table Page

LIST OF FIGURES

LIST OF FIGURES – CONTINUED

Figure Page

ABSTRACT

Vibrothermography is a non-destructive testing (NDT) method that utilizes high frequency acoustic vibrations to cause flaw faces to rub together and generate frictional heat which is then detectable using an IR camera. This testing process was first investigated over 20 years ago, however it has been slow to develop due to the lack of understanding of the mechanical processes behind the heat generation and the inability to effectively control flaw heating. Vibrothermography is particularly suitable for composite materials due to their tendency to develop subsurface delaminations between laminating plies, which are undetectable using most other NDT methods. Increased use of composite materials in structures such as airplane components and wind turbine blades has contributed to a revived interest in vibrothermography.

This paper investigates the use of the finite element analysis (FEA) method to model vibrothermographic systems. Physical samples of glass epoxy composites that contained large delaminations were tested using vibrothermography to create an empirical data set that is used to verify an FE model of a similar system The resulting surface temperatures in the FE model were compared to those observed in the physical test. Both the strengths and shortcomings of using FEA to model these systems are discussed and the proposals for how to improve the model accuracy are provided.

The second of half of the paper describes the use FEA to create thermal models of vibrothermographic systems in order to generate a detection model that will indicate the excitation time required to detect a flaw according to it's size, depth, and heat generation rate. The model also accounts for measurement noise and camera distance, and is found to be accurate for flaws with short detection times, and less reliable for those with longer times. The connection between model accuracy and detection time is explained by the inherent issue of problem conditioning. Possible resolutions to this problem are described and further work is proposed on how to improve model accuracy.

INTRODUCTION

> "*I remember my friend Johnny von Neumann used to say, 'with four parameters I can fit an elephant, and with five I can make him wiggle his trunk.'* " -Enrico Fermi

Vibrothermography is a non-destructive testing (**NDT**) method whereby a sample of material receives a high frequency excitation such that the bulk movement and deformation of the material results in frictional heat generation at any sufficiently large flaw. Additional heating may also occur due to viscoelestic heat generation in areas of concentrated stress, such as the crack tip, and due to plastic deformation induced heat generation when the excitation is sufficient to further propagate the flaw or cause tribological damage along the crack faces. This method works to test for material damage only in the form of cracks or delaminations and relies primarily on the frictional heating between crack surfaces. As the material is infused with ultrasonic vibrations, crack interfaces have a tendency to rub together, resulting in frictional heat generation. This heat is then conducted from the crack to the surface of the material where inspection with an infrared camera reveals local warm spots in the vicinity of the flaw, indicating damage. Vibrothermography is not effective for detecting other forms of damage or material flaws such as porosity, corrosion, or surface roughness where there are no frictional interfaces. However, it is more effective than many other NDT methods in finding cracks where there is no opening between crack faces, especially sub-surface cracks where plasticity effects force the flaw faces together. Also, when the material or structure can efficiently propagate high frequency acoustic waves, then a large area can be tested in a very short time with a single excitation source. This fact along with the lack of necessary material preparation to perform a test, makes vibrothermography one of the fastest potential

NDT method for detecting cracks and delaminations.

The setup in figure (1.1)[1] provides an example of a vibrothermographic test set up.

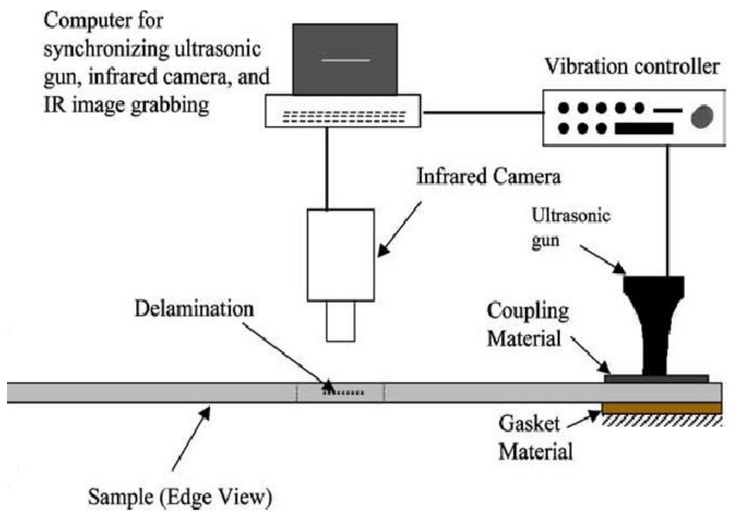

Figure 1.1: Example setup for a vibrothermographic test.

The ultrasonic gun on the right (usually a ultrasonic welder or some other piezoelectric transducer), infuses the material with high frequency low amplitude vibrations of frequency ranging between 14-40kHz. The delamination, indicated by the dotted line in the center of the material, will then begin to generate heat, as the vibrations cause opposing crack faces to rub together. The infrared camera, pictured above the material, will then be able to detect an increased surface temperature above the crack, once sufficient heat has conducted to the surface.

Vibrothermography was first studied as possible NDT method in the late 1970's[3] where it was discovered that large temperature gradients developed in the vicinity of composite delaminations when the material was vibrated using ultrasonic welders. Engineers at Virginia Tech first discovered that materials with cracks exhibited lo-

[1]This image was taken from [2] with the author's permission.

calized heating around the flaws when excited with high frequency vibrations, and that the these temperature increases could be monitored by thermographic cameras. It was immediately recognized as a promising testing method due to it's ability to test a large area in a short time, and to detect flaws that could not be found using other NDT methods, however little was understood about the physical mechanisms behind the heating. It was discovered that this NDT method was particularly well suited for composite materials with low thermal conductivities. In fact, insulating materials exhibited temperature increases that were up to three orders of magnitude higher than for conducting materials. Additionally, the size of the regions that increased in temperature was also larger for materials with low conductivity. These observations immediately lead to the conclusion that epoxy/glass composites are particularly amenable to the this testing method. Unfortunately, the advancement of vibrothermography was hindered by the lack of understanding of the physics behind the heat generation, and the non-repeatability of the chaotic vibrational excitation[4]. The non-repeatability of the excitation results in an inability to control the heating process. Early researchers were unable to develop a reliable testing scheme, and for a while, the field had lost interest.

In recent years this trend has changed, as vibrothermography gained plenty of attention as composite materials are being more widely used in a variety of applications. Advances in high resolution IR cameras and piezoelectric transducers has allowed for higher detectability of flaws and repeatability of excitation, but there still is no reliable parametric model to predict the heat generation and resultant temperature distribution for realistic delaminations. Much work has been done to better understand the mechanics of vibrothermography, however, there still doesn't exist an accepted mechanical or tribological model for these systems, as the processes behind the heat generation are inherently hidden and difficult to monitor. Some work has been done to inspect flaws after excitation with scanning electron microscopes [5] in order to verify that heat generating areas along a crack show signs of tribological damage, presumably due to frictional effect of the test. However, the results are not sufficiently conclusive to be able to infer the magnitude of the frictional forces or the dynamic processes occurring during excitation, and only serve to validate the basic theories behind the source of heat generation. In fact, the inability to monitor the flaw before or during excitation means that most of our understanding of the processes involved in vibrothermography must be inferred from temperature data away from the flaw. Furthermore, a physical model of these systems can only be verified based on it's ability to predict the temperature distributions that will develop around a crack during excitation, and to date, no excepted model exists.

Recently, more work has been done [6] to attempt to correlate certain flaw conditions with temperature data in order begin constructing a vibrothermographic model based on such data. It has been found that flaw size and vibrational stress amplitude both clearly affect the heat generation, however, a concrete functional relationship has not been established since the data is too limited and scattered. The process of generating data is also slow, as a sufficiently large quantity of flawed specimens needs to be created in a way that the flaw location and size are known. This is straightforward for through thickness flaws, as the field of fracture mechanics has developed various methods of creating and controlling crack propagation. However, one major problem is the difficultly involved in constructing and testing samples with fully embedded delaminations, which are of primary interest for composite materials, and vibrothermographic testing in general. Plenty of experiments have been performed using stress induced through-thickness cracks in materials, but little is know about flaws that have yet to propagate to the surface, which is common occurrence in composite materials, where first-ply failure begins between laminating layers. Additionally, it is difficult to efficiently produce samples with fully embedded flaws without introducing a foreign material, such as teflon film, between laminates. So very little data has been generated for these sorts of flaws. Unfortunately, as mentioned earlier, in order to determine a physical model for vibrothermographic processes, it is necessary to first generate sufficient data from which to base the model. A dependable vibrothermographic testing procedure cannot be produced without a means of modeling and predicting the heat generation process, and such a model would first need to be verified by a reasonable large body of empirical data, which currently doesn't exist for fully embedded flaws.

The first part of this paper focuses on the use of finite element analysis (FEA) to circumvent these inherent difficulties in the producing a large quantities of reliable data for vibrothermographic systems. The goal is to develop a general *method* of modeling that produces reliable data using ANSYS software. FEA methods have long been known to produce accurate solutions to complicated problems; however, they always produce *approximate* results and their legitimacy lies within the ability to correlate these solutions to analytical results and empirical data. For the case of vibrothermographic systems, there is no analytic description of the thermal and mechanical processes behind the heat generation. Instead, there is an overgrowing body of empirical data with which to verify FEA models. A few recent papers [2] [7] [8] [9] [10] have established the of use FEA methods for the study of vibrothermography, and have shown that FE results can accurately match the data from empirical tests, but it has yet to be established how reliably these models can be used to predict results and generate new data. This paper attempts to combine some of the methods used in these papers in combining an empirical test and an FEA model to generate data and compare results. The accuracy and legitimacy of the FEA model is investigated and suggestions are made regarding how to improve on the currently employed modeling techniques.

A description of a vibrothermographic test of composite samples with large delaminations is provided in the following chapter. Thermal data was recorded for excitations of various frequencies to use as validation data for an FEA model of a similar system. Using ANSY software, the finite element (FE) simulation models the heat generation and resulting temperature distributions for a 2000Hz frequency range and the results are compared to the tests. Many of the known problems in using FE analysis to simulate vibrothermographic systems are encountered and addressed. Some of these problems are tabulated below:

1. Computational Expense

   One major hindrance to the development of FE models of vibrothermographic systems is computational time required. These non-linear simulations require very small time step sizes and high mesh refinement in the contact regions which means that a single simulation of .1s excitation time can take from hours to days. This problem was only exacerbated by using the implicit solver in ANSYS, and ultimately it is recommended that software with an explicit solver, such as LS-Dyna is used. Even though the model presented in this paper used the built-in sub-modeling capability of ANSYS to shorten computation time, it was concluded that the this method was not sufficiently efficient for producing large quantities of data. Most of the recent work on using FEA to model vibrothermography has focused primarily on the transient heat generation that occurs during the initial stages of excitation, since a prohibitive number solution steps is required to simulate excitation until steady state. Unfortunately, longer excitation times are required to detect fully embedded flaws in composite materials, and so in these cases the steady state heat generation is of primary interest.

2. Frequency Dependance

   Early in the development of vibrothermography, it was noted that flaws in vibrating systems only exhibited noticeable heat generation at delimited frequencies. It was later verified that more heat was generated when the system is exited at resonance [3] due to the higher vibrational stresses. It was also proposed that, in certain cases, the flaw itself has resonant frequencies of vibration that are independent of the over-all structure and that heat generation is also increased at these frequencies. Both the physical tests and FE model in this paper use a wide range of excitation frequencies in order to confirm this phenomenon. In order to implement a effective vibrothermographic testing procedure, a intelligent selection of excitation frequency must be made in order to optimize heat generation and thus flaw detectability.

3. Localized Heating

   Even when an optimal frequency is chosen to excite a material containing a flaw, there still could be little to no heat generation along substantial portions of the crack. This has been thought to be due to a combination of causes including flaw location relative to node and anti-node locations in the resonant waveform. Areas of high vibrational stress tend to produce more heat than than lower stress regions such node locations. The FE model in this paper also exhibits extreme localization of heat generation that correlated with the experimental results in terms of the location of warming and the resulting surface temperatures. It was found that in this case, the phenomenon was due to the pre-loading of the sample as well as the boundary conditions, the results of which cause the flaw faces to separate in large regions thereby preventing frictional heat generation where the faces were not in contact.

4. Model Verification

   As mentioned earlier, the goal of the generating data using FE models is to create a relationship between flaw parameters, such as size and location, and heat generation. Unfortunately, empirical tests can only infer the heat generation based on the resulting temperature distributions, and model verification relies on agreement between the simulated and experimental temperature values. The FE model presented later correlate well in terms of maximum surface temperature increase, but it remains to be confirmed whether this means that the heat generation recorded in the simulation is sufficiently close to the heat generation in the test. This is an inverse problem of sorts where the heat generation rate must be inferred based on temperature data. In order to conclude that temperature correlations can be used to infer heat generation correlations, the inverse heat transfer problem that is implicit to this comparison needs to be examined to determine how error in the temperature data effects propagates to the error in heat generation rate.

If FEA models can be produced to reliably predict the heat generation that results during the vibrothermographic testing of a sufficiently wide variety of parametrized flaws and structures, then the next step in developing this method is to determine a optimal detection routine that increases likelihood of crack detection and minimizes the testing time required for a large structure such as a wind turbine blade. The second part of this paper works towards achieving that goal by developing a model to indicate the time required to detect flaws as function of size, depth, and heat generation rates. The model incorporates technological limitations, noise, and camera distance. The analytical solution to the heat conduction equation for a finite embedded planar heat source cannot be represented in closed form, and instead multiple numerical integrations are required to solve this problem. As an alternative, an FE model was created to simulate these systems for wide variety of flaw configurations in order to generate a data set that could be used to create a detection model. Using both static and transient heat conduction simulations, the detectability of flaws along with the excitation time required to produce a detectable temperature signature on the surface of the material are provided for each flaw configuration. A simple model is proposed to provide detection times as function of flaw size, depth, and heat generation rates for various camera distances. It was found that the problem of determining detection times is poorly conditioned for large times, and that further work should be done to enhance the accuracy of the model for these flaws.

The third chapter details a physical vibrothermographic test performed on four composite samples with large subsurface flaws. The testing procedure and results are presented, and compared to an FE model of a similar system provided in the following chapter. The results of the FE model are then analyzed for model verification, and possible improvements are proposed on how to more effectively implement FEA to simulate vibrothermographic systems. Chapter (5) includes the purely thermal models of heat generating flaws and proposes a function that provides the detection time for parametrized flaws, as well as a discussion of the error associated with flaws that require long excitation times to detect.

LITERATURE REVIEW

Quite a few papers have been published in recent years [2] [7] [8] [9] [10] that present finite element models of vibrothermographic systems, most of which serve to produce a better understanding of the dynamics behind the heat generation, while incorporating analogous physical tests for validation. This chapter will discuss the contributions from three different papers and analyze the work of the various authors.

Han et al.

Xiaoyan Han has made a few important contributions covering FE modeling of vibrothermographic systems, and one of his most interesting papers is reference [7] where the author uses finite element modeling to investigate the effects of acoustic chaos accompanied by the normal ultrasonic excitation on frictional heat generation at a flaw. The finite element model verified the empirical observations that chaotic waveforms present in vibrothermographic systems enhances heat generation and therefore flaw detectability. One fatal irony in the development of vibrothermography as a viable NDT method, is the non-repeatability of the process due precisely to the chaotic wave forms generated by the excitation source. The creation of a vibrothermographic flaw detection algorithm has been substantially hindered by the inability to incorporate the inherently chaotic response of the material and excitation source. Chaos, by definition is non-predicable and non-repeatable, which makes it very difficult to bound or characterize in a way that can provide a quantitative heat generation model. If it can be demonstrated with statistical certainty that the presence of chaotic waveforms, in addition to periodic waveforms, only enhances flaw site heat generation, then the heat generated by the application of the periodic waveform alone can be set as a lower bound in the vibrothermographic models incorporated in a flaw detection routine.

The means of creating the chaotic waveforms in the model presented in reference [7] was designed to closely simulate the hammering action of the transducer on the material. The transducer tip was modeled as a separate unattached volume from the material, which in the case of this model was aluminum. Ultrasonic vibrations were applied to this volume and transferred to the aluminum plate via contact forces. The plate and transducer would regularly lose and regain contact causing a hammering effect resulting in chaotic acoustic waveforms propagating through the plate. This hammering phenomenon was more common in early vibrothermography tests where ultrasonic welders were used as the excitation source. These high frequency impacts were sufficient to cause damage to composite materials both at the transducer location, and at the crack tip, where the high energy vibrations resulted in crack propagation. In recent years, it has been found [5] that the excitation provided by well controlled piezoelectric transducers combined with a buffer material such as leather or duct tape, has limited the hammering phenomenon as well as the resultant material damage. By forming a better understanding of the mechanics behind the additional heat generation when chaotic acoustic waveforms are present, perhaps an optimal, non-chaotic and repeatable excitation pattern could be developed that enhances heat generation and facilitates the development of a reliable vibrothermographic detection routine.

Mian et al.

Dr. Ahsan Mian authored two papers [2, 11] that combined a physical test and FEA simulation of a vibrothermographic system involving a carbon/epoxy composite plate with stress induced cracks propagating from a center hole. His paper verified both the utility of vibrothermography for composite materials and the potential of using FEA software as tool to aid in the understanding of the mechanics behind friction based heat generation. A 20KHz 40ms acoustic pulse was applied to the sample using a 1 kW ultrasonic gun. The excitation source and IR camera were sequentially triggered by a computer in order to create accurate time-history data. Though the excitation time was short, the IR images clearly demonstrated heating around the flaw. The FEA model was created using LS-Dyna software and involved both a mechanical and thermal simulation in order to determine heat generation and the resultant temperature changes, respectively. Relative nodal displacements between initially coincident master and slave nodes are compared and plotted, providing insight to the mechanical response of points along the delamination. This is a subject that is usually neglected by other presentations in the FEA modeling of vibrothermographic systems. By closely examining the relative velocities, displacements and stresses along the flaw surfaces, better surface interaction models can be created that are specific to vibrothermographic systems. Of course, care must be taken to account for the fact that such data is also the result of the chosen contact algorithm. For example, elastic slip, the relative sliding of initially coincident nodes, will still occur even when nodes are in sticking contact. This output data needs to be tabulated along with the nodal "penetration" that occurs in the numerical simulation. Though these phenomenon have some physical interpretation, they are not physically realistic and should be properly accounted for when nodal displacement data is used to interpret the mechanical response. Dr. Mian's insightful look into nodal displacements sets the stage for for future investigations into the largely unknown kinematics behind the frictional heat generation in vibrothermographic systems.

His paper [2] also looks into the transient heat generation at the flaw and compares the rates of heat generation for flaws with varying coefficients of friction. This was inspired by the empirical observation that the two cracks in the experiment exhibited different heat generation rates despite being of similar size and experiencing the same frequency excitation. It was discovered that the heat generation rate was directly proportional to the friction coefficient in this system. This conclusion naturally provides the explanation that the varying heat generation in two flaws is explainable by the differences in surface roughness, which can be quantified with the frictional coefficient. Also, although the 40ms pulse was sufficient to produce a noticeable temperature change on the material surface, the plot of energy accumulation indicate the heat generation rate had not reached a steady state value. This is common to just about every paper on the subject for two reasons: it is computationally too expensive to run simulations until steady state, and temperature signatures are apparent before steady state for flaws that propagate to the material surface. Unfortunately, the transient heat generation values are less pertinent for systems involving fully embedded flaws, since, in these cases, longer excitation times are required for detection. The heat generation values provided in reference [2] do provide a good indication as to what the steady rates would be by establishing an upper bound. It is seen in the paper that the rate of generation decays with the transient response, so at least a maximum value can be inferred.

One final aspect of references [2, 11] to recognize is the use of a laser vibrometer to determine the excitation amplitude at the transducer. The same amplitude displacement was applied as a boundary condition which allows the model to reach steady state faster, and insures a more realistic mechanical response. This detail is often neglected in similar investigations, even though it has been well established [3, 6] that the heat generation is proportional to the vibrational stresses which depend on the response amplitude. Therefore, any results and model verification are incomplete without confirming the material deformation experienced in the FEA model are reflective of the physical experiment. The results in [2, 11] are therefore strengthened by the use of the actual measured displacement, however, it is unclear whether damping parameters were set so that displacement at the flaw site also match the experiment, since the flaws are 10cm from the load source. Another way the model verification could be improved in these papers would have been to provide the temperature data from the experiment and simulation in compatible units. The experimental data is presented in terms of signal intensity and the FEA data is units of $^{\circ}C$ so only qualitative comparisons can be made.

R. Plum & T. Ummenhofer

In their paper, R. Plum et. al, [10], investigate the frequency dependence of frictional heat generation in a vibrothermographic systems through parallel empirical tests and FEA modeling. They performed tests on a cracked steel plate over a frequency range of 19-23kHz and observed that significant heating occured only for delimited frequencies. It was also discovered that some broad frequency ranges produced no noticeable heating. This same frequency dependance was observed in the composite plydrop tests mentioned earlier. It has been proposed [3] and fairly well demonstrated that a flaw will typically produce more heat at resonant frequencies of the underlying structure and the flaw itself. However, this is not universally true. If the resonant mode shape results in low stress and small amplitude respone at the flaw site, then heat generation may still be minimal. This strong reliance on proper frequency selection drastically reduces the reliability of vibrothermography as it stands today.

The FEA model in reference [10] was performed using Ansys/LS-Dyna, and their methods were used as the basis for the plydrop model presented in chapter (4). In order to overcome the long computational times for vibrothermographic systems, Plum employed a sub-modeling procedure and then a load transfer model that applied the frictional heat generation determined during the sub-modeling routine as an applied heat flux load at the crack faces in a purely thermal model, in order to avoid performing a direct coupled field analysis, which would have been computationally too expensive. A frequency sweep over 10Hz intervals was performed over the same range as the physical tests and the data was compared. This is the only paper that this author found that used FEA simulations to compare both the frequency dependence of vibrothermographic systems and the localized behavior of the heating. The FEA results qualitatively correlated with the experimental findings. Highly frequency dependent and localized heat generation was observed, and the resultant temperature changes were of the same order of magnitude.

This thorough investigation into vibrothermographic systems could be taken as a good starting point for developing FEA models to generate reliable data, however, in reference to the results discussed in chapter (4), the results are incomplete without demonstrating the mechanical response of the FEA model has accurately matched the physical system and that steady state excitation has truly been achieved after 100 cycles. With respect to the former concern, response amplitude measurements could be taken during the physical experiment, similar to those recorded in [2], in order to properly apply loading conditions and damping parameters in the FEA model. The latter concern is unlikely to have been satisfied, and so the results may depend significantly on the sampling point at 100 cycles with respect to the lower order modes. As was seen in the plydrop models, initial excitation results in the transient activation of low frequency modes, which unless over-damped, will require multiple cycles to diminish. This may not have been the case with the steel plate that was modeled in [10], however, this would have to be properly investigated and demonstrated for the results to be complete. Nevertheless, the paper focuses on some of the primary concerns with vibrothermography with respect to frequency dependence and localized heating, and serves to better explain and demonstrate these phenomenon.

THE PLY DROP SAMPLES

In order to determine the feasibility of vibrothermographic testing to locate imbedded flaws in epoxy glass composites, it was first investigated whether the method works on common delamination failure sites. One such frequent source of failure is the plydrop, which, as the name suggests, is the reduction in thickness of a composite material accomplished by reducing the number of laminated plies in a portion of a structure. This results in resin pockets or voids where high stress concentrations

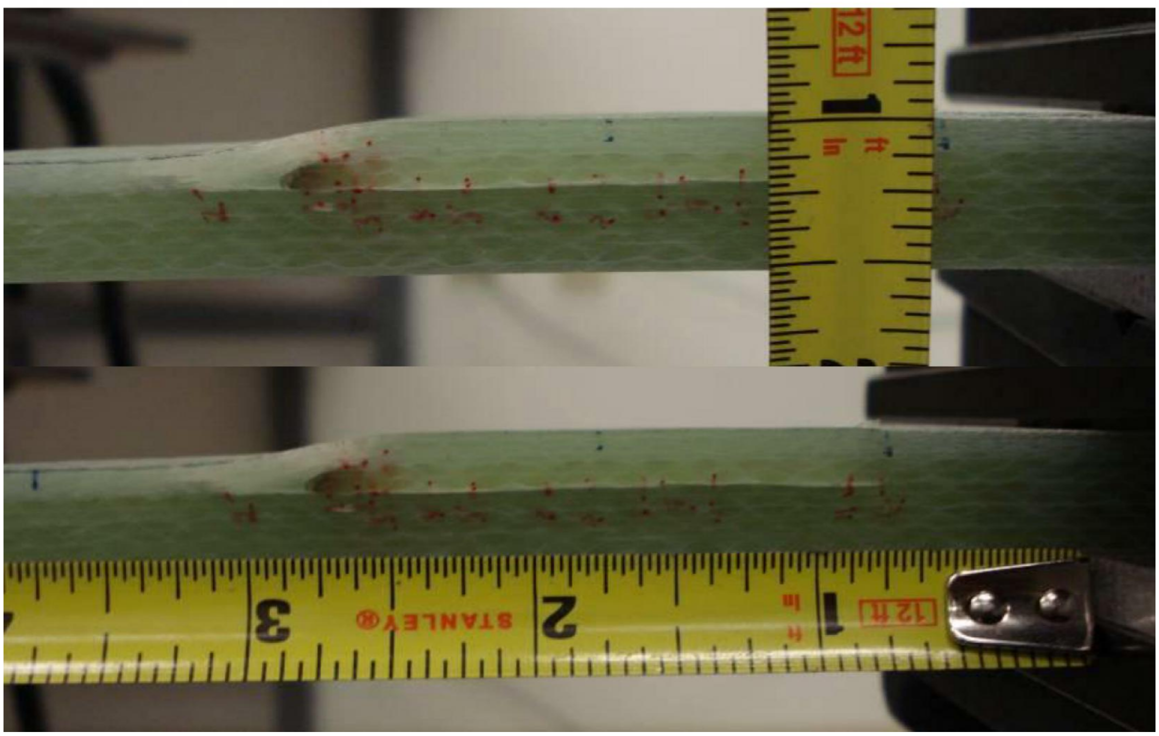

Figure 3.1: Plydrop Sample with 2.5in Through thickness Delamination. This image was provided by Resodyn Corporation and is from the report [1].

cause first ply failures [12]. These failures usually propagate between plies below the surface, and are often undetectable by visual inspection and most NDT methods. In order to verify whether vibrothermography could be used to detect plydrop failures, 4 plydrop samples were created at MSU and loaded until a delamination failure occurred and propagated from the location of the plydrop. Vibrothermographic tests were then performed on each sample at Resodyn Corporation[1] for thermal response at excitation frequencies ranging from 18kHz to 20kHz. The samples were observed from the side and top surface to verify whether the heat generated at the delamination would conduct to the surface to cause a measurable temperature change. During the test, the samples were clamped free, as shown in figure (3.1), and a high frequency transducer was placed at the free end to provide the vibrational excitation. An accelerometer was placed on the bottom of the sample directly beneath the transducer in order to record excitation acceleration amplitude. An initial test was performed on each sample to determine which frequency resulted in the greatest thermal response. The samples were then tested three times each at their respective maximum response frequency, and each test was for 180 seconds of excitation time[2]. This data was then used to validate the results of an FE model that is described in later chapters. The four plydrop samples were of similar (but not identical) geometries, and each had flaws of different sizes and apparent shapes. Additionally, they were vibrated with different driving forces and each exhibited its greatest thermal response at a different frequency.

Factors Affecting Heat Generation

These plydrop samples exemplified the primary strengths and difficulties of vibrothermography. First, it was found that the thermal response is highly dependent on the excitation frequency, with the greatest heat generation occurring over a 300Hz

[1] The tests were performed by Kyle Capp and Peter Lucon during the summer of 2011. All data was conveyed to the author in the report [1].

[2] This data can be found in [1] but will be omitted from this document

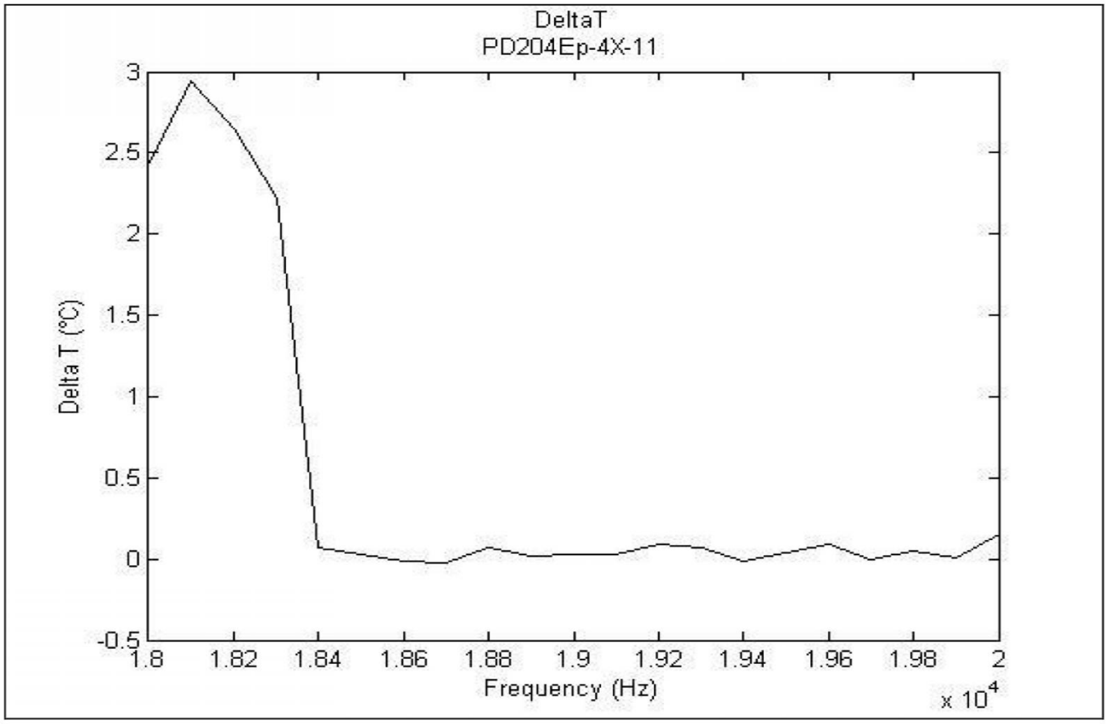

Figure 3.2: Thermal frequency response of plydrop sample. This graph can be found in [1] and was provided by Resodyn Corporation.

band that includes a modal frequency. Frequencies above and below the resonant frequency often generated no measurable heat. As a result, even a large flaw, like the one pictured in figure (3.1), would be undetectable using these methods unless a proper excitation frequency is chosen. This phenomenon is clearly demonstrated in figure 3.2 where the sample experienced a $3\,^{\circ}C$ increase in surface temperature when excited at 18100 Hz, but no noticeable temperature change was recorded for temperatures above 18400 Hz.

The existence of a such a broad frequency range where there is limited or no thermal response presents difficulties when actually implementing this testing method. In order to insure heat generation that is sufficient for detection, either the sample needs to be excited over a large enough frequency range to include at least one high-response frequency or an excitation frequency must be selected (if it exists) that will insure sufficient heat generation. It has been demonstrated [3] that heat generation is greatest at the resonant frequencies of the structure, or, if the material is sufficiently thin or the delamination near the surface, at the local resonant frequencies of the delamination itself. However, the delamination resonant frequency cannot be known without prior knowledge of the shape and location of the delamination, so it cannot be accounted for in a detection algorithm that assumes no knowledge of the existence or properties of any flaws. The structural resonant frequencies, on the other hand, can be determined during excitation based on simultaneous measurements of the amplitude of the excitation response. Therefore, it may be necessary to monitor the mechanical and thermal response of the material during a vibrothermographic test when the resonant frequencies of the system are unknown.

The mode shape of the resonant frequencies can also influence the thermal response [5]. A flaw or a portion of a flaw located near a modal node will experience less bulk movement and lower stresses resulting in lower heat generation than a flaw located in a region of higher vibrational stress, such as an anti-node location. This means that the boundary conditions of the structure, i.e. locations of clamps or supports, can substantially influence the detectability of a flaw since the mode shapes of structures are determined in part by the constraints. Consider the IR image of the plydrop sample in in figure (3.3)[3]. It is clear that the heat generation is not evenly distributed along the delamination, but instead, is localized to a small portion of the flaw. In fact, most of the flaw generates almost no heat and is therefore undetectable at this excitation frequency. The high degree of localization in this case could be due to the particular mode shape at the chosen excitation frequency. The heat generating region

[3]This image was provided by Resodyn Corporation.

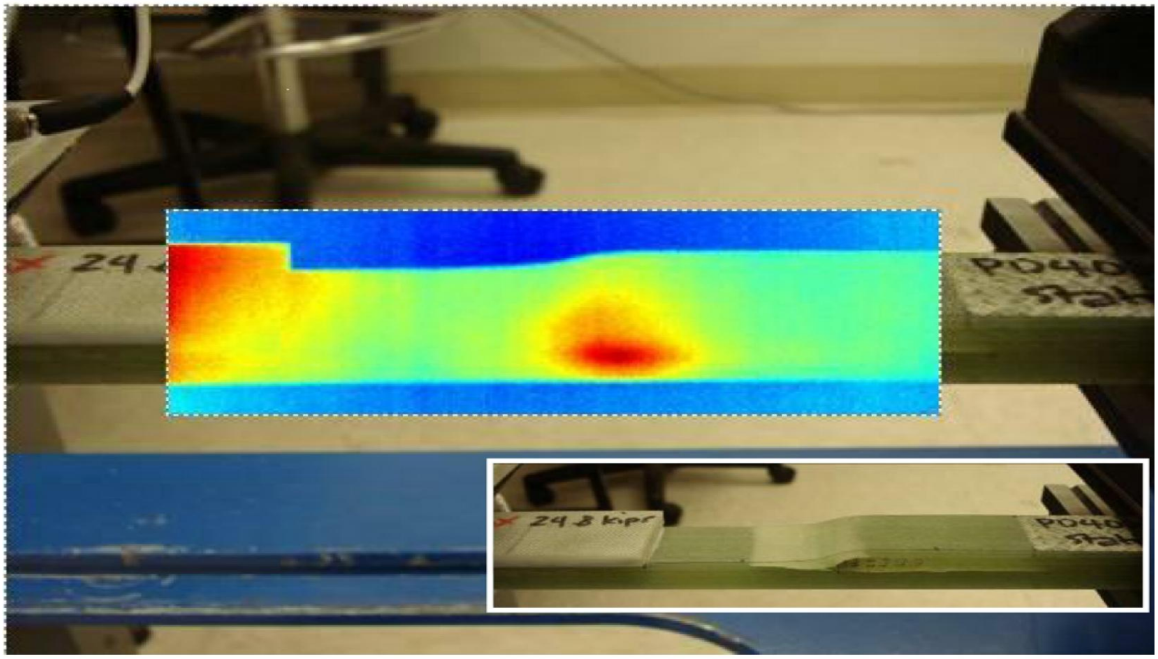

Figure 3.3: Side view of plydrop IR temperature image.

would likely occur at an anti-node where the vibrational stresses are relatively high. Of course the mode shape and node location result from the positioning of the clamp and the plydrop geometry as well as the transducer location. With this in mind, a vibrothermographic detection method should sufficiently incorporate these geometric properties of the sample in order increase the detectability of a given flaw.

The amount of damping in the structure can also drastically effect heat generation rates. A highly damped material will have a lower amplitude excitation, even at resonance, and will rapidly dissipate energy. This factor becomes increasingly important when testing for flaws that are a substantial distance from the transducer, as the vibrational energy diminishes rapidly with distance.

The thermal and mechanical properties of the material are also important factors for flaw detectability. It is suggested [3] that the most significant parameter in terms of detectability is the thermal diffusivity of the material. A material with high thermal diffusivity, such as aluminum, is a poor candidate for vibrothermographic testing, since heat is rapidly diffused away from the flaw, resulting in lower surface temperature changes. However, this paper is only concerned with a single material - epoxy/glass composites, and no tests or models were developed involving other materials.

Difficulties in Generating Empirical Data

Many flaws in laminated composite materials occur below the surface where out-of-plane geometric irregularities, like the plydrop, or matrix imperfections such as air bubbles often cause laminate first ply failure. In order to devise a proper detection scheme using vibrothermography, it remains to be determined how detectable these fully imbedded delaminations are. A proper detection algorithm should be able to predict the likelihood of detection for these flaws, yet there is little empirical data to support this process. One reason for this is the difficulty in creating test specimens with artificially introduced flaws that don't include some intermediate material, such as Teflon film to create the delamination. Other methods of creating flaws involve the repeated loading of a sample until delamination failure occurs, such as in the plydrop samples, but this process is difficult to control and replicate for a large enough quantity of samples that would be required to produce a representative data set for the flaws of interest. It is these difficulties that motivate the use of FE models to generate data that can be used to create the detection scheme. However, in order to validate the FE models, more empirical data will be required. The following chapter presents an FE model similar to the plydrop samples in order to verify whether the the numerical simulation can capture the same magnitude heating as well as the localized effects seen in figure (3.3). This model can then be used not only to improve our understanding of the mechanics behind the frictional heat generation, but also to validate the use of FEA for vibrothermographic systems.

THE FEA MODEL

An FEA model of a plydrop sample with a through thickness delamination was created using ANSYS software. The geometry was chosen to be representative of the four plydrop samples from [1], with a through thickness crack, clamped-free boundary conditions, and a sinusoidal excitation load at the free end. The delamination was modeled as 4 different but coincident areas (2 on each face of the delamination) with an identical mesh creating two sets of unconnected nodes at identical locations. The delamination was meshed with TARGE170 and CONTA173 elements. The simulation utilized ANSYS' built-in sub-modeling routines as well as its multiphysics capability. Data was gathered in 100Hz increments over a 2000Hz frequency range that included one harmonic frequency. Each simulation included 3 parts. First, a relatively coarsely meshed model was run for 100 excitation cycles, at which point it was assumed the the driving frequency response had reached steady-state. Next, a sub-model was created that included just the volume around the delamination, but not the entire length of the sample. The nodal solution results from the last 5 cycles of the coarse model were applied as nodal displacement boundary conditions on the outer boundary of sub-model. Frictional heat generation data was then gathered from the last three cycles of the sub-model, and averaged over time for each contact element. Finally, a thermal model was created with identical node and element numbering around the the delamination as in the sub-model, so that the averaged heat generation values for each element could be applied as a heat flux in the same location. The thermal model was run for 180 seconds of simulation time, and the surface temperature results were compared to the data from [1].

The Coarse Model

The coarse model is designed to efficiently determine the global steady state response of the plydrop sample to the cyclic load. In order to properly resolve the sinusoidal load, twenty time steps are required per cycle, which means 2,000 solutions steps are performed for the initial 100 cycles. If the model were highly refined around around the delamination, then the solution time would be prohibitively long. The sub-modeling technique provides a recourse from this problem by allowing the system to achieve a steady state response with a coarse mesh and applying the displacement data at steady state as boundary conditions to a refined model. The orange section in

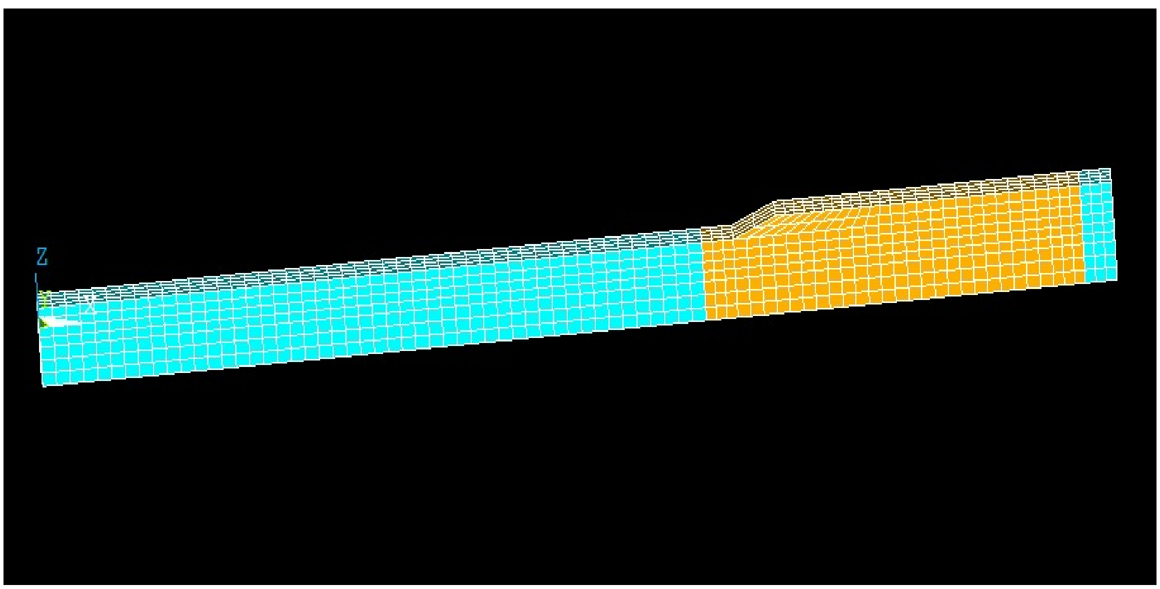

Figure 4.1: Coarse Model with Sub-model Volume Highlighted in Orange

figure 4.4(a) is the sub-model volume, and the entire collection of elements is the coarse model. As recommended by ANSYS, the element edge length for the coarse model was chosen so that the minimum element edge length was $1/20^{th}$ the wavelength at the excitation frequency. That way, the wave propagation is properly resolved. The coarse model was meshed entirely with SOLID185 elements, which is an 8 node hexahedral element with displacement degrees of freedom. In order to ensure that the dynamic response still accounted for the presence of a large delamination, the flaw was included in the coarse geometry and meshed with TARGE170 and CONTA173 elements. Figure 4.2 shows the location of the flaw. If no sub-modeling routine

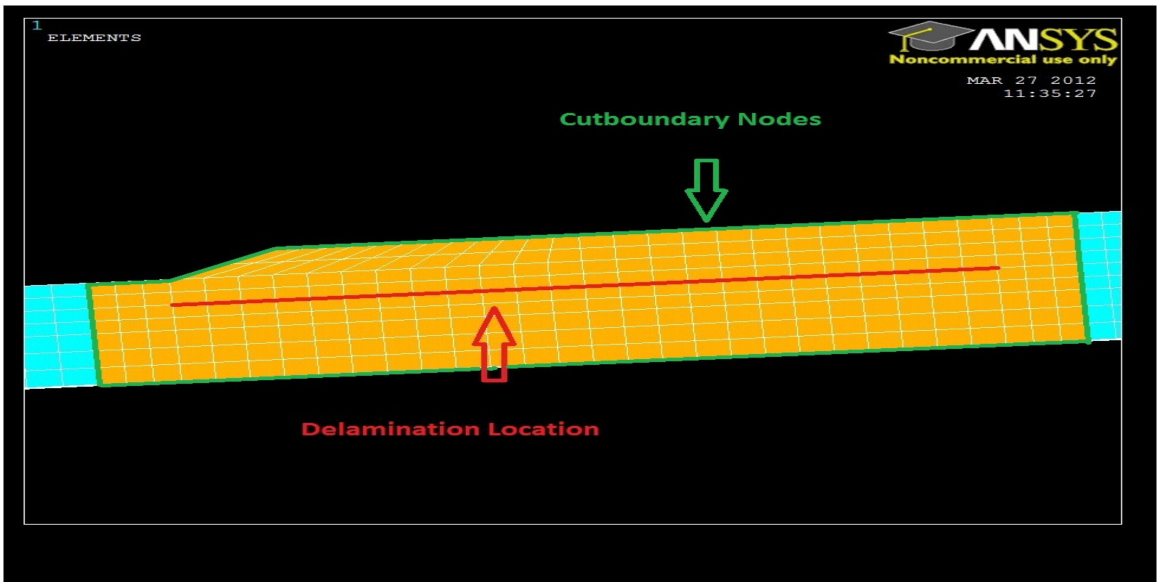

Figure 4.2: Location of The Flaw In the Coarse Model And the Cut-boundary

were employed, the elements around the delamination would need to be more highly refined in order to obtain accurate frictional heat generation data. Instead, the nodal displacement data is saved along the cut-boundary indicated by the green lines in Figure 4.2. This data is then applied to the nodes in the same locations in the refined sub-model.

Loading

The loads applied in the FEA model were meant to replicate the physical tests performed at Resodyne. A 39lbf pre-load was applied. The pre-load and the lower amplitude excitation force were distributed with an aluminum section placed across the end of the sample. This test configuration allowed for the application of symmetry along the length of the sample in the FEA model, since the load is assumed to be evenly distributed. The excitation force was applied using two different methods, both of which produced equivalent heat generation results. The first method was to apply the load directly to the nodes at the top of the sample within $1/4^{th}\,in$ of the end. The load was applied as the 39lbf preload with the addition of a sinusoidal driving force with an amplitude of 4.78lbf rms[1]. The second loading method began by first performing a harmonic analysis of the system and then applying the vertical displacement results of the harmonic analysis as time-dependent displacement boundary conditions at the loading location in the transient analysis. This way, the loading amplitude would start at the steady state value, and the first mode transient response could not be present. Both methods produced similar results, but the second method was chosen to produce the results presented later. Although the clamp described in [1] provided a compressive force on the sample, this force wasn't measured, and is presumed to provide little contribution to the results. In order to model the clamp, the nodes on the top and bottom of sample that corresponded to the clamp location were constrained for all displacement degrees of freedom.

Damping

The amount of damping present in the material has drastic effect on the results, and needed to be implemented carefully. When over-damped, the system produced very little heat as the excitation amplitude was diminished and more energy was dissipated by damping effects. Conversely, an under-damped system resulted in an unrealistically large heat generation rate, and high amplitude dynamic response. The temperature vs. frequency graph in figure 3.2 gives us an indication of what sort of

[1]The actual tests performed on four different samples used forces ranging from 4.78 to 25.93lbf rms amplitude [1].

damping constants to expect. The sudden spike in the heat generation around the resonant frequency may indicate[3, 5] that the amplitude of mechanical response in this range is substantially higher than in the region of little heat generation. This means that damping factors should be set so that the harmonic response graph has a similarly steep peak around the resonant frequencies and diminishes rapidly as the driving frequency departs from resonance. The damping ratio, ζ, for the plydrop samples was measured[2] to be between .001 - .002 in the frequency range of 16000 to 20000 Hz. However, although ζ is measurable property of the system it cannot be input directly in an Ansys transient analysis. Instead, α and β damping were implemented using the following relations

$$\alpha = 2\zeta\frac{\omega_1\omega_2}{\omega_1+\omega_2} \qquad \beta = \frac{2\zeta}{\omega_1+\omega_2} \tag{4.1}$$

where ω_1 and ω_2 were chosen to be two harmonic frequencies in the frequency sweep range. Although ζ is a measurable property of the system, α and β are not, so these damping values were verified using a harmonic analysis to determine whether the system response included a sharp peak around the resonant frequency. Figure (4.3) shows the harmonic response for the selected damping values. The range of frequencies was chosen to be centered around the harmonic peak, which was around 17400Hz.

The Sub-model

Although the element size in the coarse model is sufficiently small to resolve the high frequency wave propagation, it is not sufficiently refined around the delamina-

[2]These test were performed by Corey Cook and Kyle Kapp at Resodyn's facilities using the half bandwidth method.

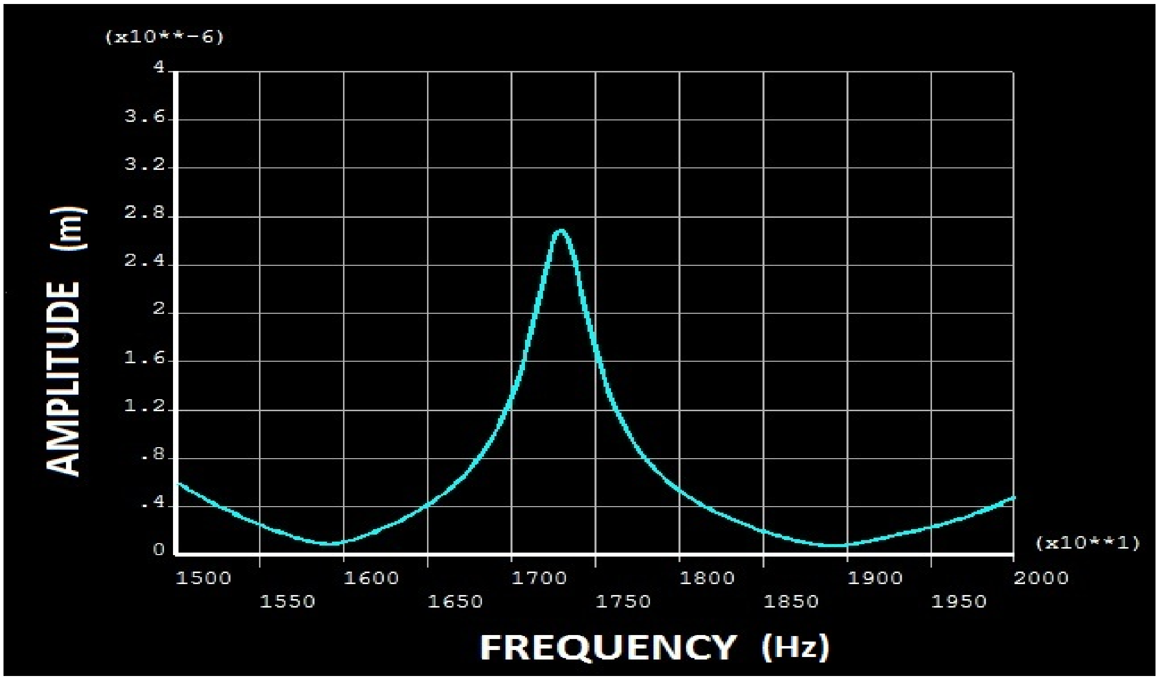

Figure 4.3: Harmonic Response of Coarse Plydrop Sample With $\zeta = .01$.

tion to obtain accurate contact friction results. As previously mentioned, we are only interested in the steady state heat generation rates, but in order to get those values, a transient analysis needs to be performed for many cycles, which would be computationally too expensive for a highly refined mesh. As an alternative, the mechanical response to the system over 100 cycles is obtained in the coarse model, and the these results are applied as boundary conditions to the sub-model. Images of the coarse and sub-model are shown in figure (4.4). The nodes along the sub-model boundary

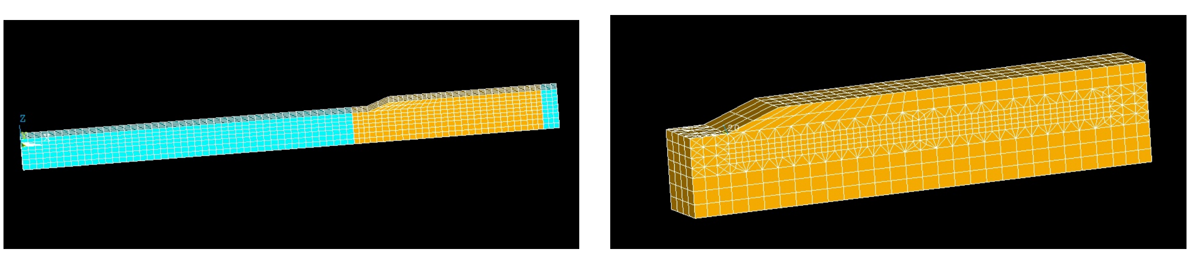

(a) Coarsely meshed plydrop volumes

(b) Finely meshed sub-model

Figure 4.4: Images of meshed coarse and sub-model volumes

share identical node numbering and locations as the coincident nodes in the coarse model, so that the coarse results are easily transferred. However, using the ANSYS command CBDOF, the program can also interpolate the results from the coarse model in the case of non-identical mesh along the boundary. Even though the node distancing along the sub-model boundary are the same as in the coarse model, the mesh around the delamination is now highly refined in order to obtain more accurate contact results. The volumes are meshed with Solid185 hexahedral elements along the delamination, and Solid186 tetrahedral elements along the transitional volume between the flaw region and the cut-boundary.

Verifying the Sub-model

Sub-modeling is common practice in static analyses where the application of a displacement boundary condition provides the same solution as the application of an external force provided that the area of interest is reasonably far from the boundary. This follows from St. Venant's principle, which basically states that all statically equivalent loads produce similar stresses when considering a region far enough from the loading point[3]. In our case, the loading is not static and so there is more room for error if the sub-model isn't properly initiated. Therefore, the results and error associated with the use of dynamic submodeling need to be more closely examined. Similar methods were used successfully in [10] to provide FEA simulations of vibrothermography.

[3] It should be noted that the loading applied in a sub-modeling routine has a stronger relationship to the coarse model than just static equivalence. In fact, if the node locations between the outer and inner model are the same then the loading should be identical. Differences do arise when the boundary mesh is refined, and interpolated displacements are applied, however even in this case the loading scenarios follow the same local distribution pattern, and similarity is stronger than just static equivalence.

A simple procedure was performed in order to verify whether the substructure response with applied boundary conditions would match the response in the coarse model. First, the coarse model was simulated for 25 excitation cycles, and then a sub-model routine was executed using the same sub-modeling region as in the heat generation analysis, but without refining the mesh, so that element and node numbering were identical between the two models. The sub-model applied the results from the last 10 cycles of coarse model as boundary conditions. Nodal displacement data was recorded and compared for all nodes along the delamination. The maximum percent error between the sub-model and coarse model at each sub-step are plotted below. By the 40th sub-step, which is the first step for which friction data is averaged

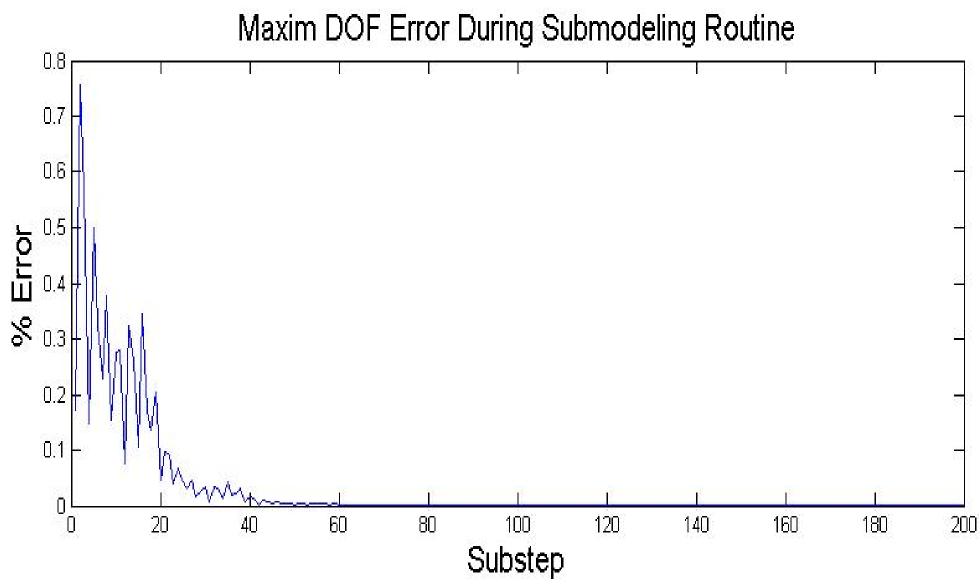

Figure 4.5: Maximum DOF error at each sub-step for a transient sub-modeling routing with identical mesh

during the sub-modeling routine, the maximum nodal displacement difference between the coarse and sub-model is below 0.0153%.

It is interesting to notice that the error appears to be in the form of a decaying sine wave with the addition of another decaying function, i.e. of the form

$$error(t) = ae^{-bt}\sin(\omega t + \theta) + ce^{-dt} \tag{4.2}$$

This should be expected as the sub-model geometry, once isolated and constrained by boundary conditions, will have an independent set of eigenvalues and natural frequencies that are not present in the coarse model. These natural modes are exited upon initiation of motion, but quickly decay, while the driving excitation remains. A Fourier analysis of the error graph in figure (4.5) revealed a broad spike around 130,000 Hz. A modal analysis of the sub-model constrained along boundary for which coarse model constraints are applied, revealed that the first three modal frequencies ranged from 120,000Hz to 134,000 Hz. It is likely that the error plotted in figure 4.5 is due to the excitation of at least one of these three modes during the sub-model routine. Nevertheless, the error is small enough after 40 sub-steps (two excitation cycles) that it is unlikely to have a significant effect on the results. What this demonstrates is that loading applied to the entire model is is equivalent to the applied boundary conditions in the sub-model in the region of the crack. Of course, the sub-model is refined around the delamination, which would certainly effect the results as any refinement would, however as long as the loading scheme is the same, then it is expected that the refinement only enhances accuracy.

It also remains to be verified whether 100 excitation cycles are sufficient for the heat generation rate to reach steady state. It was initially assumed that lower frequency modes present in the transient response would contribute little to the rate of heat generation, and that frictional heat generation would reach a steady state along with the drive frequency response amplitude. As it turns out, this is not the case.

In order to verify the transient heat generation response, a course model was run for 2000 excitation cycles, with a 5 cycle sub-model routine performed every 100 cycles in order to sample the heat generation rates during the transient response.

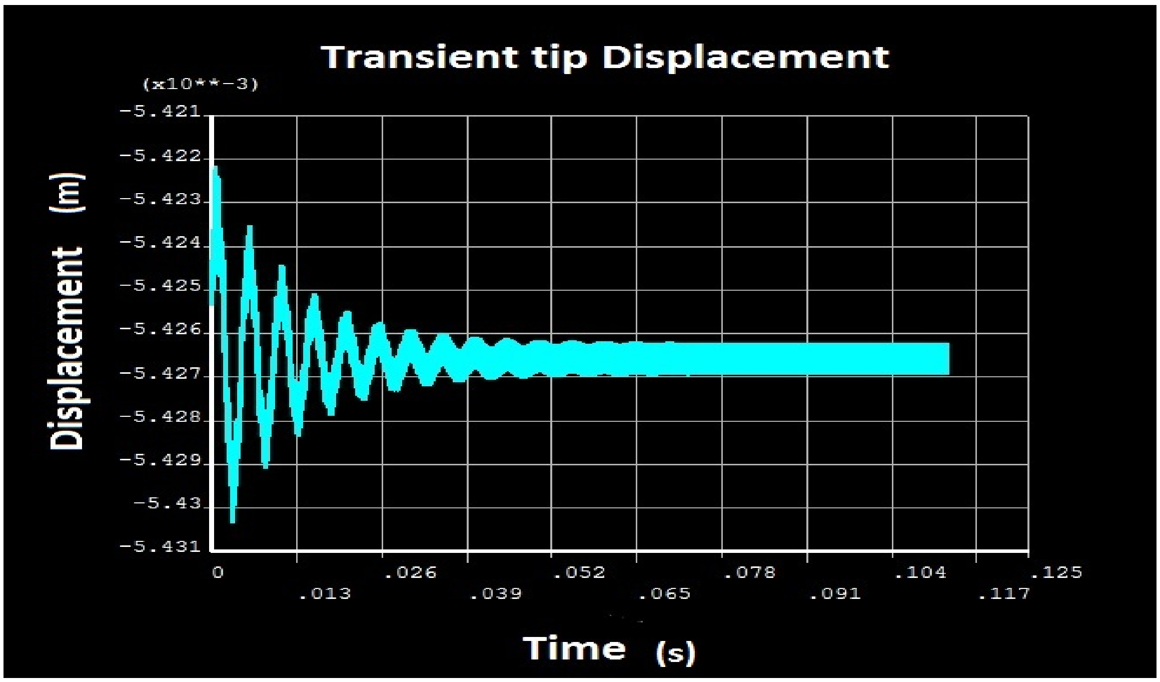

Figure 4.6: Transient response at node on free end

The plot of tip displacement and the heat generation over the 2000 cycles are shown below. The lower frequency response exhibited in figure 4.6 is expected during any transient analysis. A modal and harmonic analysis was performed of the plydrop sample and it was found that the first modal frequency is around 200Hz, and that the sample harmonic response at this frequency is over 2 orders of magnitude greater than the harmonic response at the modal frequency in the sweep range. Therefore, it is expected that this lower frequency dominate the transient response, even when the excitation frequency is equal to the higher modal frequency. This behavior is clearly exhibited in figure 4.6. A fast Fourier transform of the response revealed that dominant transient frequency seen in the graph is in fact 200Hz.

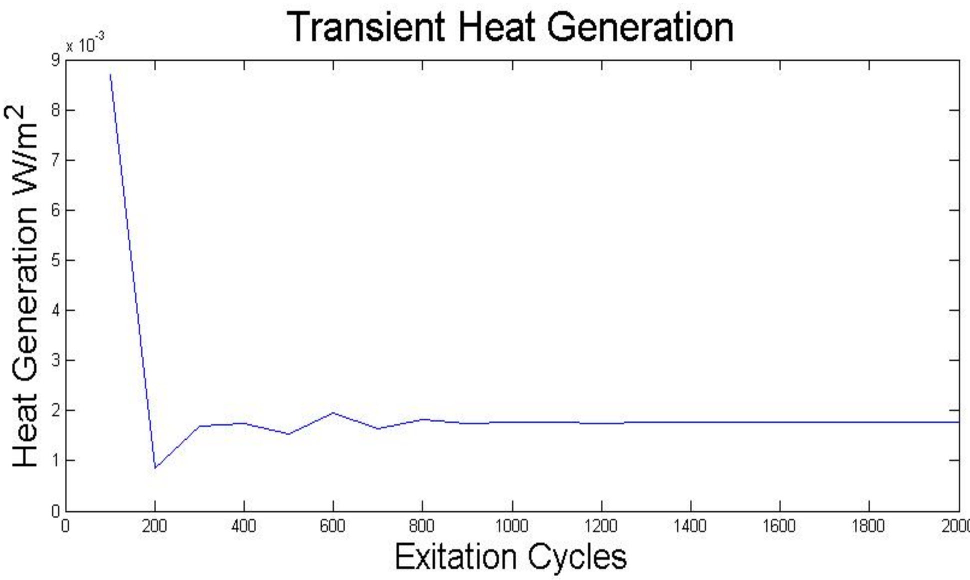

Figure 4.7: Heat generation sampled every 100 cycles

It is clear that steady state heat generation is achieved once lower mode transient frequencies are sufficiently damped out. This occurs after about 1000 excitation cycles, or .05s of simulation time, after which the changes in heat generation are less than 0.1%, and the 200 Hz response has completed 10 full cycles and is almost completely diminished. It can be concluded that in order to strengthen the accuracy of the model, the coarse model should be carried out to 1000 excitation cycles, or 10 complete cycles of the lowest modal frequency with the highest harmonic response, before initiation of the sub-model. If a 20000 Hz frequency sweep is performed at 100Hz intervals, then the resulting computation time would be at least 5 times as long and would take weeks to complete. Perhaps using Ansys/LS-Dyna's explicit solver could expedite the computing process so that this method can be used to efficiently generate more data.

Sub-model Results

Because the empirical data for the plydrop samples mentioned earlier is all in terms of surface temperatures, the temperature distribution resulting from the frictional heat generation needs to be examined in order to verify the model. That data provided in [1] was for 180 seconds of excitation time, so a direct coupled field analysis for a 180 second simulation with 20kHz excitation would require 72,000,000 solution steps. If each step took just one second to solve, then the problem would still require over two years to complete. This obviously isn't an option, so a load transfer coupled-field approach was taken. To do this, the frictional heat generation results derived from the sub-model are averaged over time for each element and then applied as constant values to a thermal model with identical element numbering along the delamination. This method implicitly makes two assumptions. The first is that the rate of heat generation has reached steady state when data is gathered. The second assumption is that application of a constant average heat source provides the same results as the actual time dependent periodic heating that would result from the vibration induced frictional heat generation. The first assumption is dealt with above, where it demonstrates that heat generation rates do reach a steady value, but only after 1000 excitation cycles. This second assumption is handled in reference [10], where it is demonstrated that the low amplitude periodic heat generation results in nearly the same heat distribution as the constant averaged heat source. Even though the true heat geneartion acts as a periodic pulse as the sample vibrates, the thickness of the sample and the insulatory thermal properties of epoxy glass composites tend to override the thermal pulsing, as the resultant heat storage and temperature increase are large compared to the amplitude of the heat generation cycles.

The Thermal Model

As mentioned in the previous section, the averaged contact frictional heat generation rates for each element was applied as an element flux in a thermal model of the entire plydrop sample with identical mesh numbering around the delamination as in the sub-model. In order to maintain the same mesh numbering, the delamination and it's contact elements needed to be included. Since contact elements accept element surface heat flux as an input load, but target elements do not, perfect thermal contact was modeled between the two surfaces by selecting an arbitrarily large thermal contact conductivity. This resulted in an evenly distributed heating along the two delamination surfaces in the regions of frictional heat generation. The volume was assumed to dissipate heat by convection with a convective coefficient of 10 W/m^2K, and since symmetry was utilized, the symmetric plane was modeled as being perfectly insulated. The heat flux was applied for the full 180 seconds and temperature data was recorded for the nodes along the top surface of the sample. Solid70 elements were used to mesh the model, which only have nodal temperature degrees of freedom. The delamination was modeled to be in closed contact along the entire length, even though it was found that during preload and excitation a gap did exist. It is assumed that this would have negligeable effect on the results.

Results

The frequency sweep results are plotted in figure (4.8). The maximum surface temperature increase of about 9 $^\circ C$ is in good correlation with data from [1] where a maximum temperature increase among the four samples was 10.6 $^\circ C$. Additionally, just as expected, the maximum temperatures are highly frequency dependent with a

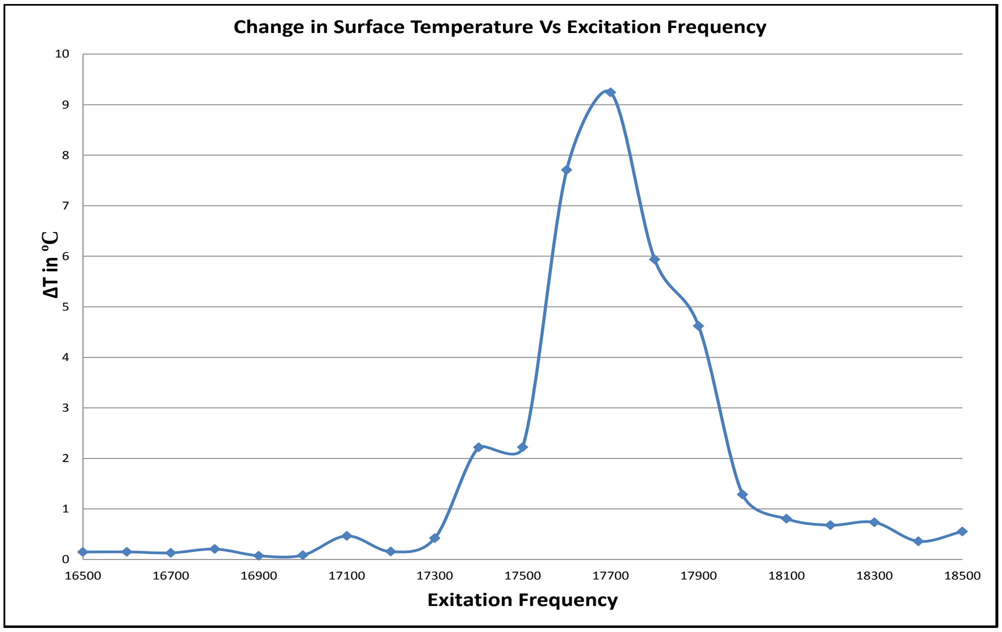

Figure 4.8: Plot of maximum change in surface temperature after 180s simulation time.

large spike centered at 17700Hz, and very little temperature change for frequencies that were over 300Hz above or below this frequency.

Additionally, the localized heating and the resulting temperature distribution was also captured by the simulation, which further validates the model. Comparing figures (4.9) and (3.3), it is seen that both the FEA simulation and the laboratory tests revealed highly localized heating in the region directly beneath the plydrop and very little heat generation elsewhere along the delamination. The reason for this can be better understood by examining the contact status along the delamination for a full excitation cycle. Each excitation period in the sub-modeling routine incorporated 40 sub-steps, which translates into two sub-model sub-step for every one coarse model sub-step in order to ramp the applied boundary conditions. Figure (4.10) displays the contact status for the delamination for 8 of the 40 sub-steps of the final sub-model

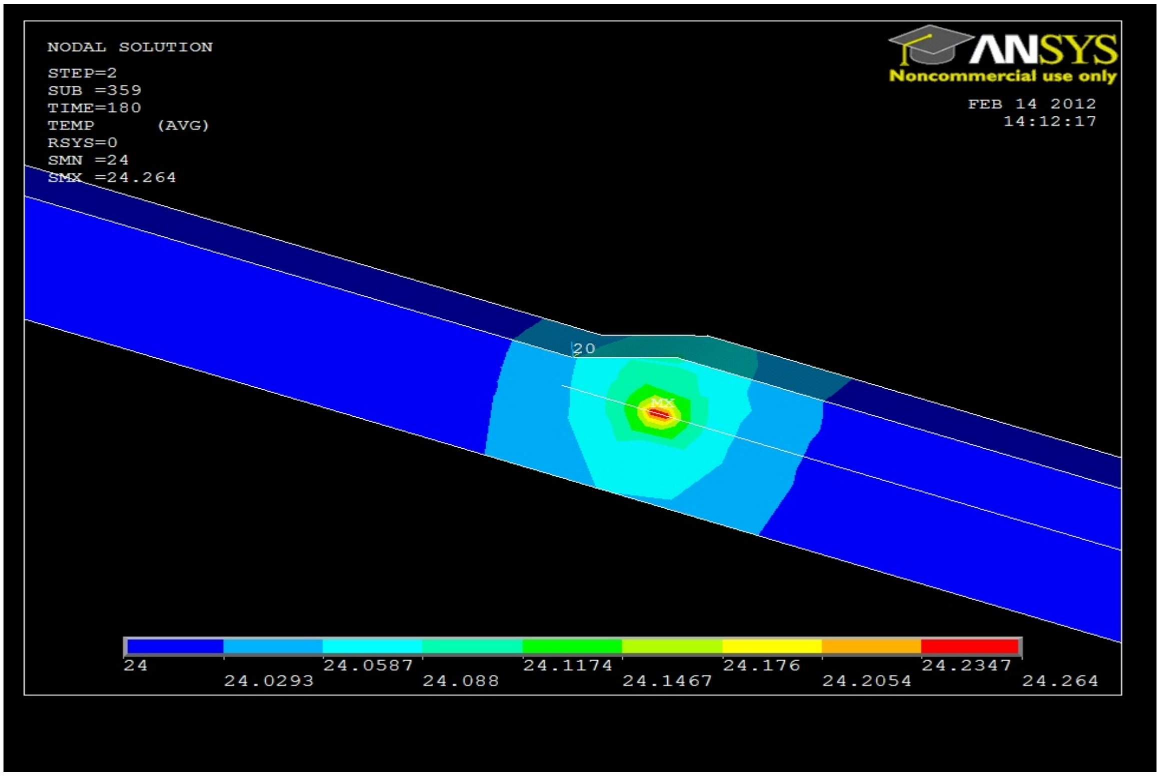

Figure 4.9: Temperature distribution in $^{\circ}C$ after 180s simulation time.

cycle. The first thing to notice are the large yellow colored regions on the left and right hand side of each image. This is where the delamination is in so-called "near field contact" which means that the flaw faces are close, but not touching. Of course, without contact, no frictional heat generation can occur. As it turns out, the faces lose contact in the region during the static preload, and the excitation amplitude is never great enough to close the gap. This explains the localization of the heat generation seen in both the physical tests and the simulation. Perhaps by reducing the preload or increasing the transducer force, the gaps could be closed at least momentarily during each cycle which may result heat generation over a larger region. However, the effects of varying these parameters were not considered here.

The images in Figure (4.10) also have a large red region which indicates where flaw is in "sticking" contact, meaning that the faces are touching, but there is no

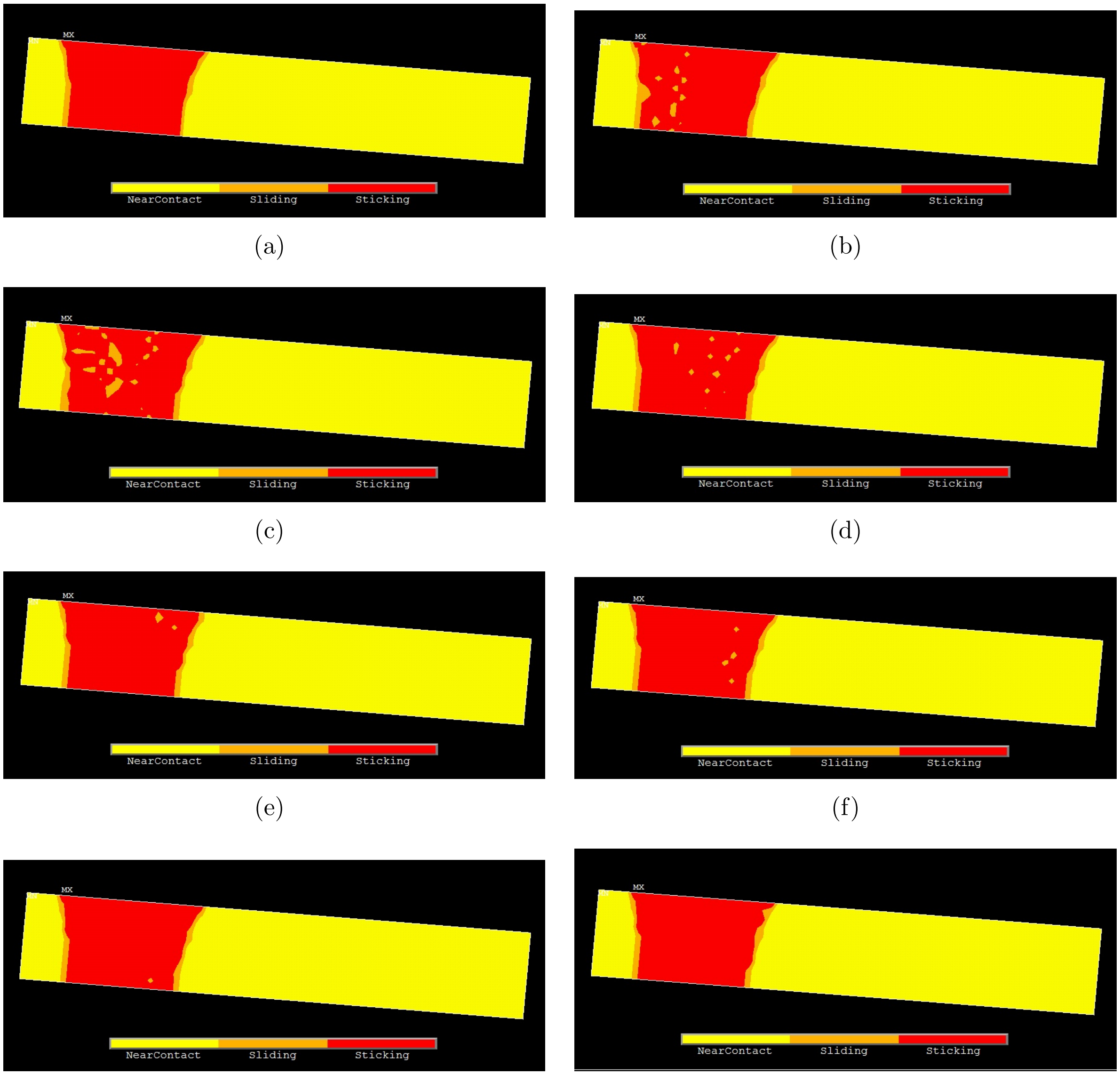

(g) (h)

Figure 4.10: Contact status for 8 out of 40 sub-steps in each cycle.

relative sliding. In particular, images 4.10(a) and 4.10(h) show when the flaw faces are almost entirely either in near field contact or sticking contact so that no heat is being generated except at the region of transition between the two states, which appears as an orange band on the right and left hand sides of the sticking area. These bands are areas of relatively low contact forces and though they are in sliding contact here, the heat generation is very small. Images 4.10(b) - 4.10(f) show small regions within the area of sticking contact where the portions of the delamination are momentarily in sliding contact. This is only time during each cycle that any area within the red region transitions from sticking to sliding, and it where most of the heat generation occurs. These six frames comprise just 15% of a an excitation cycle, so that for most of the time, there is no appreciable heat generation.

The determination of contact status is the direct result of two contact options: the choice contact algorithm, which in this case was the augmented Lagrangian method, and the friction model, which by default was the Coulomb model. The contact algorithm and friction model combine to determine the contact forces between the surfaces and the contact status. By changing the many parameters associated with both options, the contact state along with the heat generation can be drastically altered. It remains to be demonstrated whether this combination of contact models accurately describes the surface interaction in vibrothermographic systems, however, it is clear that these methods will produce results that correlate with empirical observations.

One point of disagreement between the ANSYS model and the empirical data is in the actual frequencies at which maximum temperatures were recorded. The four plydrop samples from [1] exhibited a maximum thermal response in range from 18200Hz, to 19800Hz, however the FEA model resulted in very little heat generation in this region. This is most likely due to the fact that the material properties that determine the harmonic modes were input as representative values for epoxy/glass composites, and probably didn't match the actual sample material properties, such as Young's modulus in the three cardinal directions, or the density. This would result in a disparity between the natural modes of the actual samples and the model. The model probably had a lower stiffness or higher density than any of the samples, resulting in lower natural frequencies. Another explanation for the discrepancies could be due to the fact that although the drive excitation amplitude had reached a steady state, transient response of the coarse model had not been damped out after 100 cycles. As the excitation frequency is incrementally increased, the time at which 100 cycles is completed is slightly earlier than for the previous frequency. Returning to figure (4.6), it is clear that after 100 cycles mechanical response is dominated by the lowest frequency mode. The frequency dependance of the thermal response seen in figure (4.8) may be explained by where the 100 cycles for each frequency lies on the response curve. Unfortunately the computational time and memory required to thoroughly plot the heat generation during the transient response is beyond the resources of this paper. Further investigation needs be taken into the subject in order to provide more conclusive results.

Conclusions About the Plydrop Model

The purpose of the plydrop simulation was twofold. First, it needed to be verified whether FEA simulations using ANSYS would be able to accurately match empirical data for vibrothermographic systems. This has been established to some extent in a handful of publications ([2, 9, 10] are just a few) that have demonstrated that numerical modeling using other widely available software is a potential tool for simulating vibrothermographic systems. The second purpose was to build on the methods presented in these papers while developing a general modeling technique that could easily be transferred to other sample geometries and flaw configurations that are specific to common composite structures, such as wind turbine blades. This way a large body of data can be generated in order to develop a reliable and efficient vibrothermographic detection routine that maximizes the probability of detecting flaws over a large area.

Although the data presented in this paper is promising, it alone is insufficient for achieving both goals, and should be received with skepticism.

Finite element modeling is powerful and verifiable numerical method for obtaining accurate solutions to complicated mechanical problems. In a small displacement, small stress, linear, static analysis the solution to the system of equations describing the system converges on the exact analytic solution as the mesh becomes increasingly small. Unfortunately, in the case of a transient analysis with frictional contact there usually doesn't exist a "exact" analytical description that can be used to compare to the FEA solution. That is to say, there is not transient mechanical or frictional contact analog of Hooke's law from which the system of equations are built. Instead, Rayleigh damping, Coulomb friction, and augmented Lagrange contact are employed in large part due to mathematical convenience. Although each of these constructions has some empirical basis, none are considered to provide an exact description, and their use is justified by the fact that in many situations they provide adequate solutions when compared to experimental data. In the case of frictional contact in vibrothermographic system, not only is there no generally accepted theoretical formulation with which to compare the system as described in an FEA simulation, but there is also no means of directly measuring the frictional forces, or heat generation in a physical test; the only information available is the surface temperature distribution. It is well known that inverse heat transfer problems are ill-posed, and so determining the heat generation rates based on experimentally determined temperature data may not be reliable. However, for that case of vibrothermographic systems, the boundary conditions are known along with the surface temperature data, so the inverse problem corresponding to this system, may not be as unstable as other inverse heat conduction problems where the boundary conditions are not known and only internal temperature data is available. Nevertheless, there really isn't any means of validating the quantitative results obtained through FEA modeling of vibrothermographic systems, except in terms of surface temperature distributions. The validation data for the plydrop model is made by comparing the temperature data at single point in the Ansys simulation to the maximum temperature measured in the physical tests. These comparisons alone may be sufficient to quantitatively validate the heat generation rates obtained from the FE models.

As mentioned earlier, the other aspect of the FE model that needs to be considered is whether Rayleigh damping, Coulomb friction, and augmented Lagrangian contact provide an accurate description of the physical system. Systems described using these formulations have proven to be accurate for a wide variety of problems; however, in this case of modeling a vibrothermographic system, the results are highly dependent on the local accuracy that these methods provide. Many of the parameters associated with these methods are not physically measurable material properties, such α and β damping coefficients, or the normal and tangential contact stiffness constants. Even the coulomb friction model, which is a reasonably accurate description of simple frictional systems, may not accurately model the frictional state for small displacement, high frequency periodic motion. In the case of the plydrop model, we are able to adjust multiple parameters to produce the desired temperature results, which are based on a few coarsely developed data points - namely the damping ratio and the maximum temperature data. But with such large arsenal of free parameters, success was virtually guaranteed in terms of model verification. The default Ansys formulation provides two adjustable damping parameters, three friction parameters, and at least three other relevant and impactful contact parameters. With this many knobs to turn and only one solution output to compare with empirical data (the maximum surface temperature after 180s) it would be premature to conclude that the system has been well modeled and that these methods can accurately be applied to predicatively develop data for an arbitrary system.

In order to develop an FEA modeling method of vibrothermographic processes that can be more confidently applied other systems, there are a few more variables that could reasonably be measured and matched by the models, such as the steady state tip displacement amplitude over a frequency range, which could be accurately measured using a high frequency vibrometer. Additionally, the frictional constants can be selected based measured data for reciprocating friction between epoxy/glass delamination surfaces. Also, as mentioned in section (4) the coarse models should be carried out to at least 1000 excitation cycles, or until a steady state mechanical response is achieved. Because the plydrop samples had near surface delaminations that spanned almost $1/3^{rd}$ the sample length, the mechanical response of the system was impacted by the presence of the flaw. However, if smaller, fully embedded flaws are modeled in larger plates, so that the presence of the delamination has negligible impact on the system response, then a properly selected sub-model region could be used to generate data for a large number of flaw configurations within the plate using the same coarse model solution, which would greatly diminish computation time, by not requiring an independent coarse model for each flaw.

Recommendations

In order for the FEA models of vibrothermographic systems to serve any purpose, they must be able to accurately predict the heat generation rates for a variety of flaws. Simply matching temperature data in a single case is rather straightforward, since, as mentioned earlier, there are multiple adjustable parameters that strongly influence the results. The goal should be to develop a systematic basis for selecting those parameters based on the material and structural properties of system being modeled. This section proposes a few tests that could be performed to enhance the accuracy of the FEA models.

Friction Model

The rate of heat generation at a flaw is dependent on two things: the frictional properties of the flaw and the mechanical response of the system containing the flaw. There is very little literature pertaining to the frictional properties of epoxy/glass composite delaminations. Some research has been done [13] to investigate the coefficient of friction for carbon/epoxy delaminations, where it was found that the fiber orientation has a strong effect on the frictional properties. The coefficient of kinetic friction, μ_k, for this material ranged from .2 to .5 depending on fiber layout relative to the motion and between the two delamination faces. It was also found that μ_k increased with normal force and in some cases decreased with each frictional cycle. By default, Ansys uses the Coulomb friction model, which describes dynamic friction using the following formula

$$\mu = \begin{cases} \mu_s & \text{if} \quad \tau \leq \mu_s \sigma_n \\ \mu_k \left(1 + \left(\frac{\mu_s}{\mu_k} - 1\right) e^{-DC \times v_{rel}}\right) & \text{if} \quad \tau > \mu_s \sigma_n \end{cases} \tag{4.3}$$

where τ is the tangential frictional force, σ_n is the normal force, and DC is the decay constant that determines how fast μ approaches μ_k according the local relative velocity, v_{rel}, between the surfaces. One aspect of this frictional model is that the surface will transition from slipping to sticking anytime $\tau \leq \mu\sigma_n$, at which point no heat generation will occur. In the plydrop model, this transition occurred every excitation cycle in the area of heat generation (see figure (4.10)), as the relative magnitudes of the normal and tangential friction stresses momentarily passed the threshold defined by μ. In one paper, [2], it was shown that raising μ would resultantly raise the rate of heat generation, however, this will not always be the case with the coulomb friction model since sliding may not occur at all if μ_s is too high. Other friction models have been utilized in similar simulations, such as in [8], where the arc-tangent Coulomb friction model was used. However, this model is similar to the coulomb friction with the exponential decay described in (4.3), except that sticking is simulated when the relative sliding velocity goes below a predefined threshold.

The coefficients of friction are important not just because they determine the heat generated by a node in sliding contact, but also because they define when a node transitions between sliding and sticking contact. The figure (4.11) shows the ratio of frictional stress to normal stress for element along the delamination for the

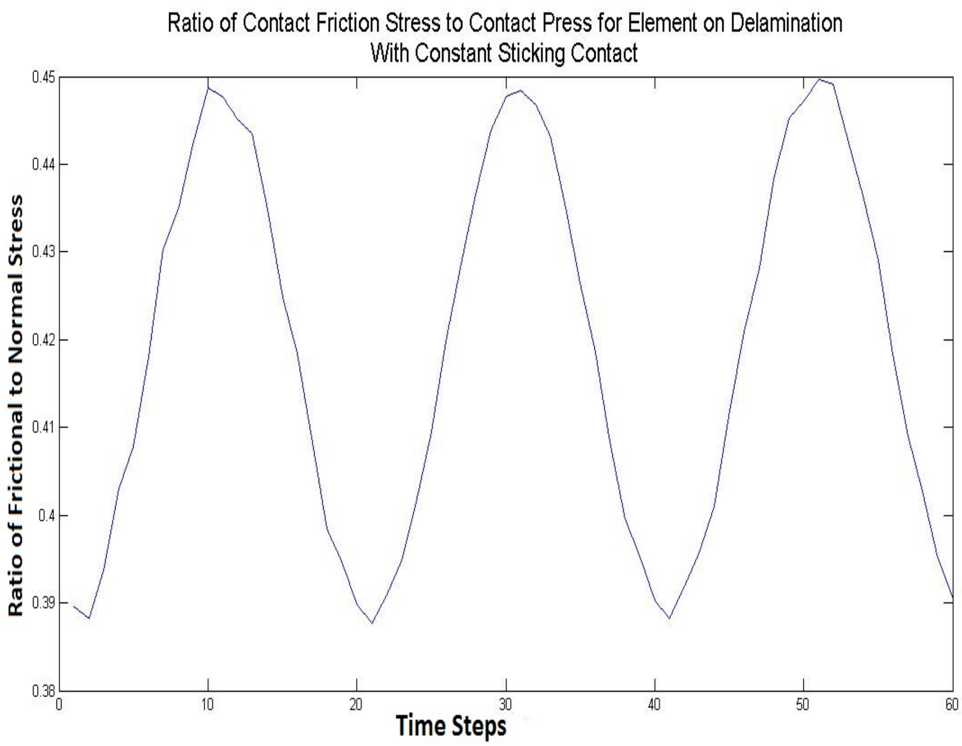

Figure 4.11: Ratio of frictional stress to normal stress given by Ansys contact element output SFRIC and PRES.

last 3 excitation cycles of the simulation, when data is gathered. This element never exceeded the critical stress ratio of .45 defined in the model, and as a result it was constantly in sticking contact and contributed no heat. Had μ_s been set to a lower value, the sliding would have occurred during at least part of each cycle, which would result in frictional heat generation at that location on the delamination. Conversely, lowering the coefficient of kinetic friction would result in lower heat generation at those nodes that were already in sliding contact. Therefore, it is unclear exactly how varying the friction coefficients used in the Coulomb model will effect heat generation in a crack without some knowledge of the dynamic state of stress during vibration, since changing the values of μ_s, μ_k, and DC can raise or lower frictional heat generation depending the ratio of τ_f/σ_n at each node. Because of this, it is important to select values that properly represent the given materials in order to increase the accuracy of the model.

One testing method described in [13] to determine friction coefficients for various carbon epoxy delaminations could be identically performed to determine these properties of glass/epoxy delaminations as well. In order to properly utilize (4.3) three frictional constants are required, namely the static coefficient of friction, the kinetic coefficient of friction between surfaces with high relative velocities, and the kinetic coefficient of friction at an intermediate velocity in order to determine the Ansys contact real constant DC. Tests for delaminations with various fiber orientations should be performed in order to get an idea of the range of possible friction coefficient values. A proper selection of the frictional constants should result in a more accurate solution.

Mechanical Response

The rate of frictional heat generation is closely linked to the vibrational amplitude of the system and the stress amplitudes at the flaw [6]. Higher amplitude vibrations typically result in greater heat generation, and so the FEA model should be certain to reasonably predict the mechanical response of a system. The vibrational response depends on the material properties like orthotropic elastic moduli and density which were chosen in the plydrop model as representative values for glass/epoxy composites. But it also depends on the damping properties, which are more difficult to quantify. A transient structural analysis in Ansys uses Rayleigh damping constants to form the damping matrix C in the system equation

$$M\ddot{\mathbf{x}} + \underbrace{(\alpha M + \beta K)}_{C}\dot{\mathbf{x}} + K\mathbf{x} = \mathbf{f} \tag{4.4}$$

Selecting C to be a linear combination of the mass and stiffness matrices is more a matter of mathematical convenience than physical law. Nevertheless, Rayleigh damping has proven to provide adequate solutions for a variety of problems and is the only built-in damping option in Ansys for transient analyses. If the damping ratios, ζ_j and ζ_k are known for two modal frequencies, ω_j, ω_j, the coefficients α and β can be selected to satisfy the following

$$\begin{aligned} \alpha + \beta\omega_k^2 &= 2\omega_k\zeta_k \\ \alpha + \beta\omega_j^2 &= 2\omega_j\zeta_j \end{aligned} \tag{4.5}$$

A damping ratio ζ, for a particular frequency is property of the material, boundary conditions, and geometry of the sample, and can only be determined by physical tests. It is recommended that in parallel to any vibrothermographic simulation, an actual sample of the same material and geometry is tested for for at least two damping ratios as well as for the vibrational amplitude in the frequency range of interest, which in this case was from 17-20kHz. That way, the parameters α and β can be chosen and adjusted until the simulated vibrational response amplitude more closely matches the empirical results. Otherwise, the resultant heat generation will be more of an arbitrary artifact of the poorly modeled mechanical system, than a true representation of the physical process. If it can be assumed that the presence of a delamination doesn't significantly effect the response characteristics of the model, i.e. a small crack in a large plate, then a harmonic analysis can be performed to efficiently determine the response amplitude for a wide range of damping values[4].

Other Unknown Parameters

Even when the mechanical properties of the system and the geometry of the flaw are known, there are other inherent flaw conditions in addition to the frictional properties, that likely cannot be measured, but will have an effect on the heat generation rates. Two properties in particular will be discussed briefly here: flaw closure and large scale asperities. As mentioned in [6], variations in these properties will appear as scatter in measured data for otherwise identical flaws in terms of size, location and geometry, however, it is possible to use FEA modeling to determine how each property effects the results.

Flaw Closure

Most delaminations initially involve cracking of the matrix material which is brittle and thus undergoes little plastic deformation. However, in some cases there will be appreciable amounts of plastic deformation or material deposition that serves to hold the flaw faces apart or possibly force them together. The initial surface conditions

[4]In Ansys, a harmonic analysis can only be performed for linear systems. If the model contains contact the the initial contact setting are fixed as constant values for the analysis, and so a delamination will not be properly accounted for. In the case of the plydrop sample, the delamination spans a large portion of the sample geometry, so the results of a harmonic (or modal) analysis need to be used with caution.

may substantially effect heat generation, and should be considered when determining the detectability of flaws using vibrothermography. Contact closure can be adjusted in Ansys in a number of ways, the first of which would simply be to build the model with a small separation of the flaw faces, as in reference [10]. However, for very small separation or initial penetration, the real constant CNOF can be adjusted to impose initial contact closure or separation by offsetting the contact surface by a specified amount. It may prove useful to determine how variations in the initial contact conditions affect the overall heat generation and flaw detectability. By running simulations for various values of CNOF, it may be determined how much initial flaw closure can account for the uncertainty in any characterization of detectability based on other flaw parameters. In the case of the plydrop model, no variations in CNOF were considered, and the flaw was always modeled as being initially closed with no penetration.

Large Scale Surface Asperities

Microscopic surface roughness can be accounted for in the Coulomb friction coefficients, but larger scale asperities that involve out-of-plane displacements that are many orders of magnitude greater than the relative sliding distances of flaw surfaces may have effects that are not captured by the friction model both in terms of local heat generation and the overall relative motion of the delamination surfaces. The plydrop model incorporated a routine that would randomly move the contact nodes in pairs in order to generate the "rough" surface, as seen in Figure (4.12). The degree of roughness, i.e. the maximum distance that nodes were displaced was parametrized so that the surface contours could range from perfectly smooth to the maximum roughness that wouldn't cause element shape violations, which in this case was about .2mm. Ultimately, it was decided that for the data provided in this paper, no large

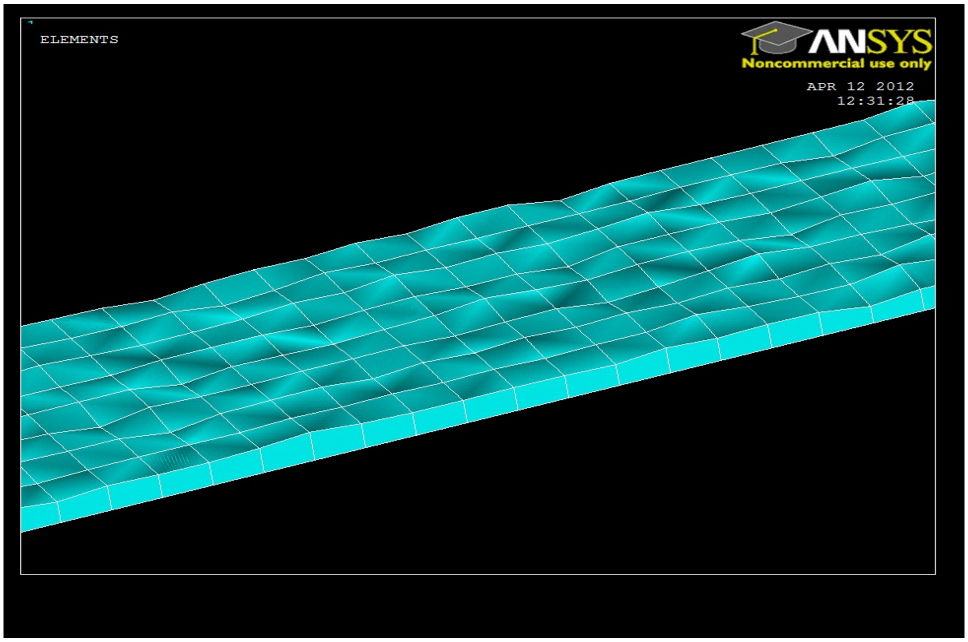

Figure 4.12: Large surface asperities generated by moving individual nodes.

asperities would be incorporated, since there was no basis from which to choose the degree of roughness. Instead, two perfectly flat areas were used to model the delamination areas. However, it remains to be investigated exactly how large-scale roughness would effect the results. A realistic flaw will rarely form a perfect plane, since out-of-plane contours in the glass will guide the direction of flaw propagation. It is expected that local changes in the surface normal direction will affect the ratio of normal to shear stress between the flaw surfaces, which in turn affect frictional heat generation as well as the contact status (i.e. sliding or sticking contact). In order to quantify the effects that large scale surface roughness has on heat generation, multiple simulations should be run with varying degrees of roughness. This information could be used to better understand the sources of scatter in the empirical data, and, along with flaw closure, may help determine the upper and lower bounds of heat generation for a flaws whose global geometric properties, such as size and depth are known, but not these local flaw characteristics.

THERMAL HEAT GENERATION/DETECTION MODELS

In order to develop a vibrothermographic detection algorithm, it first needs to be determined how long it would take to detect a flaw according to its size, depth, heat generation rate upon excitation, and the distance between the IR camera and the surface. A finite element thermal model was created in ANSYS to generate data for various combinations of the above parameters, and the Matlab curve and surface fitting tools were used to generate a model for detection times based on the data. Over 7000 data points were generated by permuting through each parameter. The goal was to develop a function that would indicate how long it would take to detect a change in surface temperature caused by sufficiently large variety of heat generating flaws. Additionally, the data is also used to determine the practical limits of this testing method in terms of flaw size, location, and heat generation rates. If enough data is generated from friction based vibrothermographic heat generation models, like the plydrop model discussed in the previous chapter, then those results can be combined with these purely thermal models to determine a reliable detection routines, as well as the limits of this testing method.

The following sections individually describe each of the variables under consideration and how they are expected to affect the results. Next, a simple model is proposed for determining flaw detection times and detectability based on these variables. The inherent uncertainty of the model is then addressed in terms of problem conditioning for different flaws and possible improvements are proposed.

The IR Camera

One reason that vibrothermography has received so much attention in recent years is due to advancements in IR camera technology. Commercially available cameras can easily detect temperature changes as small as 15mK, allowing for detection of flaws that would be undetectable with older technology. It has been shown that a highly sensitive camera focused on a non-reflective surface can detect even the minute amount of heat generated by flaws with edge-lengths as small as .5mm [6]. Unfortunately, if the material has a low emissivity, then reflected radiation from environment will generate noise that is orders of magnitude greater in amplitude than the camera sensitivities. This problem was addressed in early on [3] by painting test surfaces black, which vastly reduced the noise by raising surface emissivity. However, this may not be an option in commercial applications of vibrothermography when the structure being tested cannot be painted. Nevertheless, if an easily removable, non-toxic, thin and thermally conductive flat black coating can be found that is inexpensive and simple to apply, then an application of this coating would make flaws far more detectible in wind turbine blades, airplane wings, and other traditionally light colored and reflective composite structures. Until then, the detection algorithm needs to account for noise that is at least $.5\,^{\circ}C$ in magnitude, and comprising areas equal to 100 square pixels in the camera, in order to overcome the problem of false detection due to radiation reflection.

This is where camera distance is crucial. If the noise threshold is quantified in terms of camera pixels and the surface area corresponding a pixel decreases as the camera is placed closer to the material being examined, then the actual area over which a flaw would need to create a $.5\,^{\circ}C$ temperature rise is also reduced. This means that smaller flaws become more detectible, and all flaws can be detected faster for closer camera distances. Unfortunately, this comes at the cost of also reducing the total area being viewed by the camera, so that flaws beyond the periphery of the camera lens would not be detected. Any vibrothermographic detection routine should then select the camera distance and placement carefully in order to optimize flaw detectability and minimize total detection time for an entire structure. When determining camera distance, other variables such as vibrational wave attenuation also need to be closely examined, since there is no point in having the camera field of view larger than the material area over which vibrations have propagated with sufficient amplitude to cause heat generation at a flaw.

IR noise, for the purposes of vibrothermography, needs to be characterized by temperature and surface area. This study uses a 100 pixel area as a rule-of-thumb for the noise magnitude in terms of area. The surface area of the material that comprises a hundred pixels is based on the following formula that is specific to the camera used in the plydrop tests mentioned in previous section:

$$A = 100 \times \frac{2d\tan(\theta_w/2)}{p_w} \times \frac{2d\tan(\theta_l/2)}{p_l} \tag{5.1}$$

where d_c is the camera distance, θ_w and θ_l are the lens angles in two orthogonal directions, and p_w, p_l are the number of camera pixels per image in the same directions. In order to confidently indicate a positive detection, the surface area over which the temperature of the material has heated should be greater than A. This means that positive detection area is proportional to d_c^2, and, as will be shown later, this strongly affects flaw detectability.

The FEA Model

An FEA model was created using ANSYS software that determine the detection times for various flaw sizes, depths, and generation rates, as well camera distance. Originally, plate thickness was also incorporated as a parameter, however it was found that for a flaw at a given depth from the surface, changes in plate thickness below the flaw resulted in little change in detection time. The model incorporated a

5in x 5in x 1in plate and automatically iterated through different combinations of the previously mentioned parameters. At each iteration, a static analysis was first run to determine at which camera distances, if any, the flaw would be detectible at steady state. Again, detectability was defined as an increase in surface temperature of .5K over an area of 100 pixels in size for the various camera distances. If it was determined that the flaw was detectable at steady state for at least one camera distance, then a transient analysis was executed to determine the detection time, which is the time until the detection criteria is satisfied. The FE model used a circular flaw with a circular detection area in order minimize the effect of flaw geometry on the results, which may have complicated the data. Figure (5.1(a)) shows an example volume generated for the case of a single camera distance. The small circle in the center of the

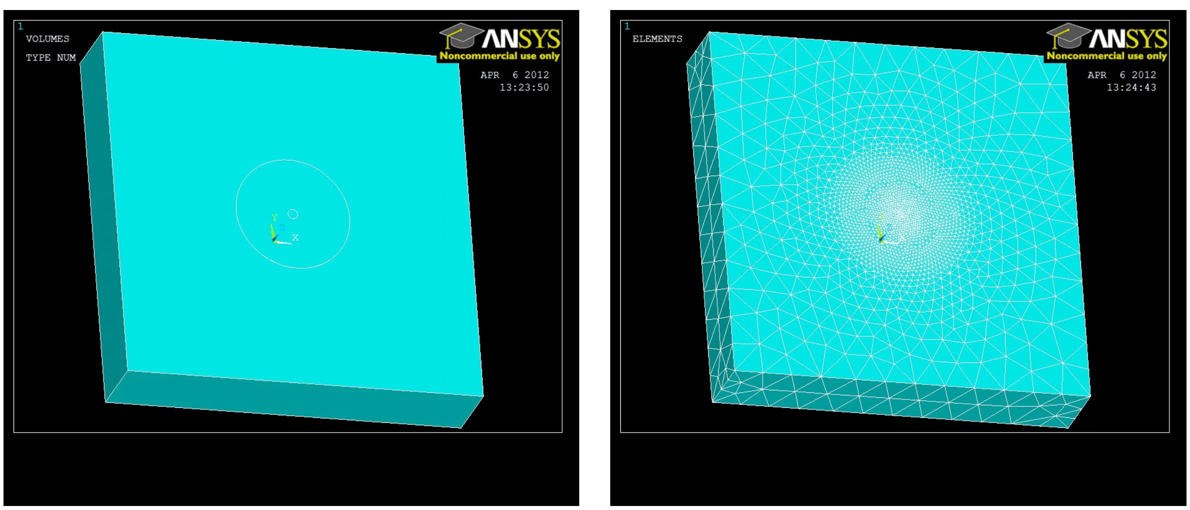

(a) FEA model volume with one search area on top

(b) Meshed volume with nodes along search line

Figure 5.1: Images of the ANSYS thermal model volumes and mesh.

volume identifies the detection criteria area for a particular camera distance. Because there is a circular line there, ANSYS automatically places nodes along the line, so that detection is determined when the temperature of those nodes rise by $.5\,^{\circ}C$. When multiple camera distances were used, there was series of smaller concentric circles, each corresponding to a camera distance, and ensuring node placement on the edge of each search area. The larger ring indicates the flaw size. The actual flaw is modeled as an area embedded in the volume. A constant heat flux was applied to the flaw to simulate heat generation. Figure (5.1(b)) shows the meshed volume, with node placement along the inner circle.

If it was determined that detection occurs at steady state, then a transient analysis was performed for a maximum of 30 minutes of simulation time. During the transient analysis the results were checked intermittently to determine whether any detection criteria have been satisfied. Once all detection criteria were satisfied, then the time of detection was recorded for each camera distance, and the transient analysis was terminated. If one or more criteria have not been satisfied after 30 minutes of simulation time, then the transient analysis was still terminated. Any flaws that were undetected after this time, were assigned a detection time of -5 so that they can easily be eliminated from the data during the model fitting procedure. If the flaw failed the steady state test for a any camera distance, then detection time was recorded as -1 for that distance. This procedure was repeated until each predetermined combination of flaw size, depth, generation rate, and camera distance was covered. Multiple runs were executed for various ranges of the parameters, in order to generate data from the full spectrum of detectible flaws, while also determining the boundaries of detectability. A single run generated up to 6200 data points, for various flaw sizes, depths, generation rates and camera distance depending on the predetermined range for each of these parameters. A sample contour plot of solution data for a single run is shown in figure (5.2).

The material properties were chosen to be representative values for glass/epoxy composites. The density was chosen as $\rho = 1876 kg/m^3$, the heat capacity as

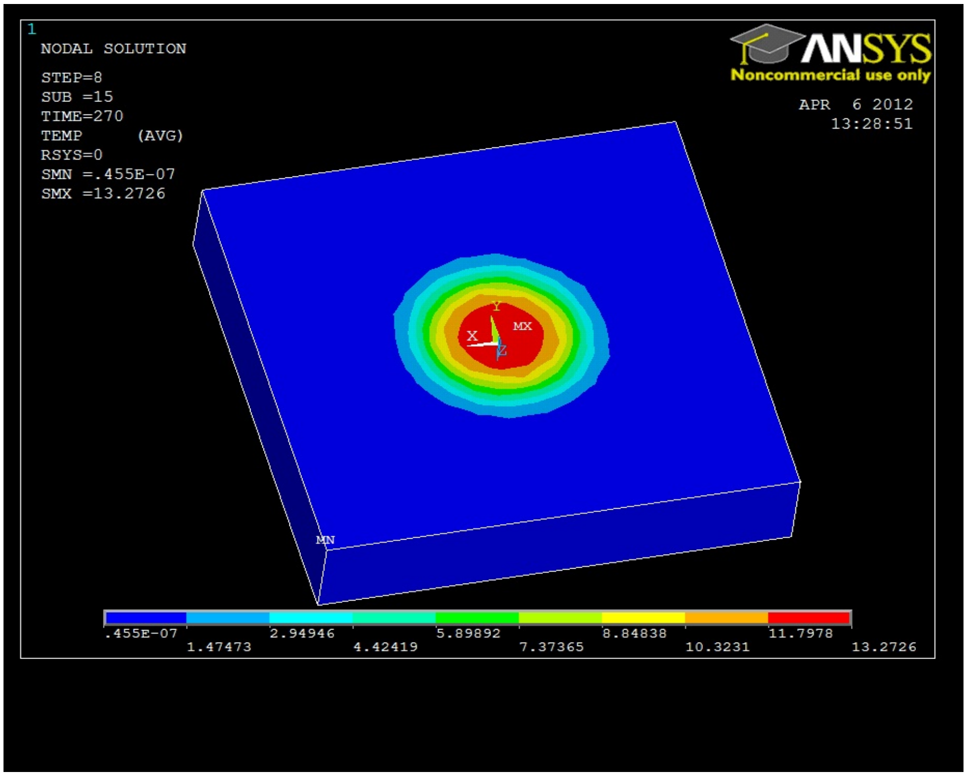

Figure 5.2: Temperature contour plot in $^{\circ}C$.

$C = 879J/kgK$m, and heat conductivity $k = .44W/mK$. Although fiberglass composites will certainly have orthotropic heat conductivity, no data was available from which to determine the orthotropic values. The isotropic thermal conductivity used in the model was supplied by Resodyn Corporation, based on their own tests, and a review of recent literature. If it is determined that heat flow in glass/epoxy composites is not accurately matched by the careful selection of a single isotropic thermal conductivity value, k, then further work would be required to see how the orthotropic thermal properties would affect the detection times, and to determine how to account for these properties in a detection routine. Additionally, even if heat flow in glass/epoxy composites can be modeled as isotropic values with reasonable accuracy, the choice of k will certainly affect the detection times and detectability of flaws, and may still need to be accounted for in a detection algorithm. For the purposes of this investigation, all material properties were left constant.

Time step size and element size were optimized with respect to detection times. A model was created with intermediate flaw size, depth and generation rates, and mesh refinements were performed until detection times failed to change within a time step. Next, the same model with the optimized mesh was run for varying time step sizes up to 2s, and the results never changed to a value greater than a single time size. The final time step remained at 2s, because a coarser step size would result in lack of changes in detection times as the parameters varied between iterations, when the detection times were less than 60s. In fact, this problem still occurred for the flaws at depths of .05in and .1in and large generation rates. In these cases, varying the flaw size often led to no change in detection times, as the difference in time must have been less than time step. However, in reality larger flaw with a fixed generation rate in W/m^2, will always result in an earlier detection time.

Curve Fitting

The goal of generating the thermal data was to generate a function that would determine a detection time based on any realistic combination of the model parameters, that is, a function of the form

$$T = f(H, d, s, A) \tag{5.2}$$

where T is the detection time, d is the depth, H is the generation rate, s is the flaw area, and A is the detection area. Of course, when starting a curve fitting routine, there is an infinite number of possibilities for the form f, so some procedure must be undertaken to begin to limit the set of potential functions. To that end, the first step was to fix three of the parameters and see how f varies with each parameter individually. That would give at least a hint as to how that parameter would appear in the final function. Also, only functions of at most 2 free parameters were considered, since any more could easily result in false positive fits.

Generation Rate

By fixing depth and flaw area, 10 data points were generated in order to determine a single variable function of the form

$$T_g(g) = f(g|a, d, l) \tag{5.3}$$

for $s = 1in^2$, $d = .5in$ and A the detection area corresponding to a camera distance of 36". It is intuitively clear that as the generation rate rises the detection time will diminish. Also, as the generation rate approaches some small value, then the detection time should rise rapidly. A clear candidate is function of the form

$$T_H(H) = \frac{s}{H^p - b} + c \tag{5.4}$$

In truth, it should be expected that as $H \to \infty$ the detection time $T \to 0$, however, the set of generation values used were only for the limited range that would provide detection times of less than 10 min or greater than 30 seconds, so the asymptotic behavior wasn't perfectly captured by the data. By allowing a constant $c > 0$ in the regression and setting $b = 0$, a better fit was obtained, but extrapolation will only be accurate for reasonably small values of H, which is in units of W/m^2. This is fine for the purposes of vibrothermography, and the frictional heat generation at a delamination is unlikely to exceed the values used to generate data. Another simplification was obtained by restricting p to integer values, so that b and c are the only free parameters for each selection of p. Setting $p = 2$ provided the best fit and the resulting model is

$$T_H(H) = \frac{2.7 \times 10^5}{H^2} + 50 \tag{5.5}$$

A plot of the data an the curve fit is given in figure (5.3). It should be noted that this

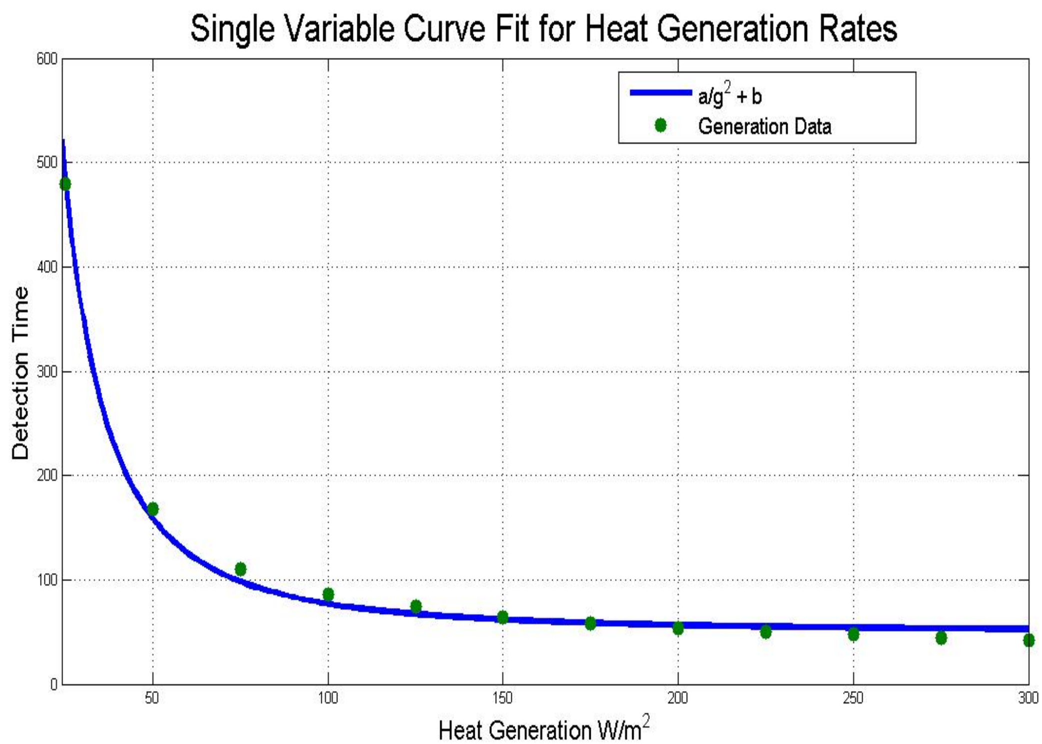

Figure 5.3: Curve fit for heat generation data with other variables fixed.

cannot be equal to an analytic solution to the problem. Given a flaw size and depth, there will be a minimum non-zero value for H such that the flaw is only detectable in the steady state, but never before.

<u>Flaw Size</u>

The next parameter to consider is flaw size. Once again, intuition tells us that a larger diameter heat source will result is shorter detection time. A simulation was run to collect data for flaws ranging from $s = .25in^2$ - $3in^2$, each with a generation rate of $H = 125W/m^2$, and a depth, $d = .5in$ in a $1in$ plate. An accurate fit was obtained for a function of the form

$$T(a) = \frac{0.009719}{s - 0.00011} + 94.47 \tag{5.6}$$

Where s is the flaw area in m^2. Although this function has three free parameters, one will be removed later when area and generation are combined into a single variable in order to create a surface fit that incorporates flaw depth as well. Figure (5.4) provides a plot of the best fit curve for the data.

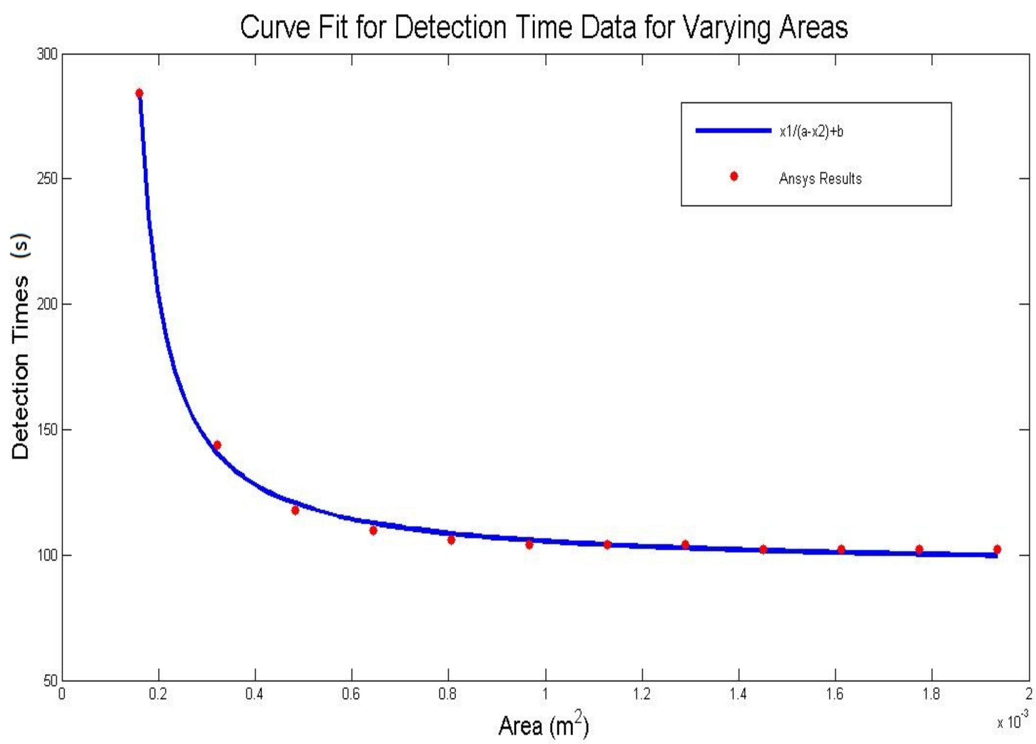

Figure 5.4: Curve fit for flaw size data with other variables fixed.

Combining Variables

In order to utilize Matlab's built in surface fitting tools[1], which only allows for at most 2 variables, area and generation were combined into a single variable. Various polynomial and fraction combinations were created and plotted with flaw depth as a second variable to create surface plots. The first guess was the simple multiplication:

$$\zeta = sH^2 \tag{5.7}$$

since the individual curve fits for the area and generation were involved the two respective variables raised to the same powers as in (5.7). Though other possible combinations were tried, this one ultimately provided the best fit once depth was incorporated.

Again, intuition motivated the role that depth would play in the surface plot. The deeper the flaw, the further the heat must travel before causing the requisite surface temperature change, and the greater the volume of material that must be heated. In fact, since the heat propagates in 3 dimensions, it is logical to guess that the detection time will be proportional to the volume of material that needs to be heated. This volume will be proportional to the depth of the flaw raised to the third power, since the heat will propagate in all directions. A natural choice, then, for the function of detection time based on three geometric variables was

$$T(d, \zeta) = \frac{p_1 d^3}{\zeta} + p_2 \tag{5.8}$$

[1]It was beyond the temporal resources of the author to create a multivariate non-linear regression m-file in Matlab, but that would have been the preferred method.

which proved unsuccessful. Eventually, after attempting various other functions, it was found that the following simple modification to (5.8) provided an accurate fit:

$$T(d,\zeta) = \frac{p_1 d^3}{\zeta} + p_2 d = p_1 \frac{d^3}{sH^2} + p_2 d \tag{5.9}$$

Where p_1 and p_2 are free variables. The R^2 value for this fit was .9847 and the RMS

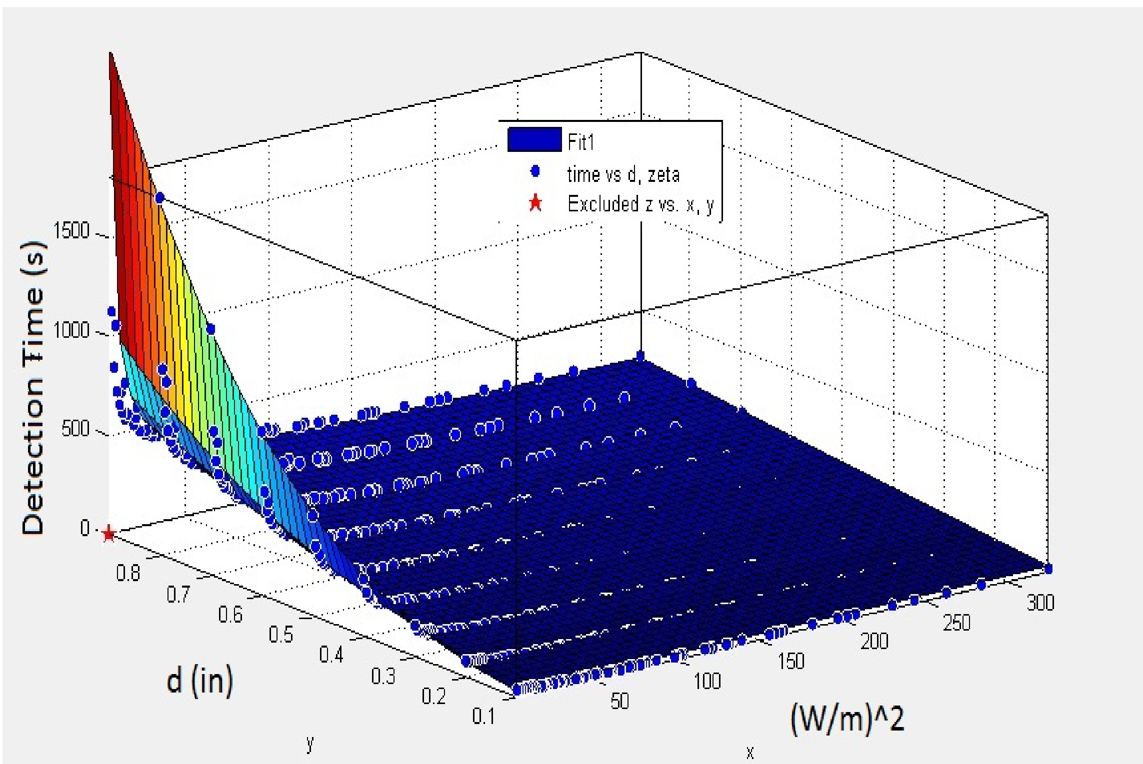

Figure 5.5: Surface fit for variables d and $x = \zeta$.

Error was 23.58 seconds. It was found the model (5.9) matched the data better for flaw configurations that resulted in faster detection times. A plot of the error for each value of flaw depth and ζ is given in (5.6). It is clear that in the upper left corner of the plot, where the depth is $.9in$ and ζ is small (i.e. a small combination of area and generation rate) the error is substantially higher. However, for shallow cracks with large ζ values, i.e. those on the right hand side of (5.6), the model (5.9) tends to predict the detection times with reasonable accuracy.

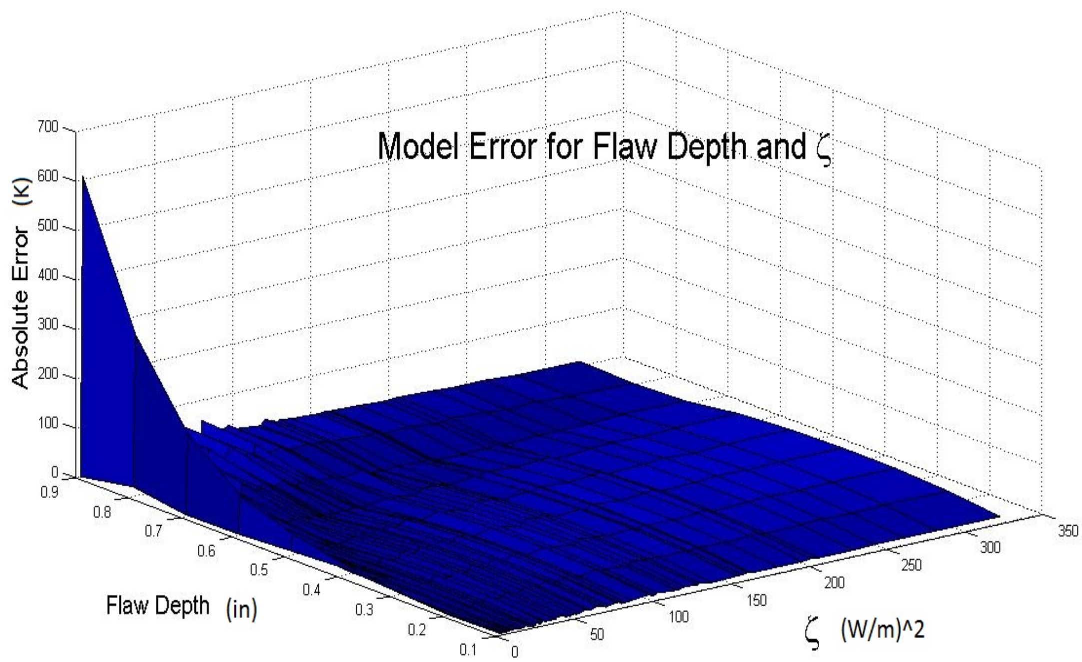

Figure 5.6: Surface fit for variables d and $x = \zeta$.

Camera Distance

After settling for the detection model (5.9) it remained to be verified whether this same relation would hold for other camera distances, and what effect varying distances would have on the parameters p_1 and p_2. Recall that as the camera is moved further from the material being tested, the surface area, A, corresponding to 100 pixels increases according to equation (5.1). In the FEA model, a positive detection is indicated when all of the nodes within a circle of radius, $r_c = \sqrt{A/\pi}$ have risen by $.5\,^{\circ}C$. As the camera is moved further from the object, r_c also increases and therefore a longer time is required to heat the area, resulting in longer detection times. In order to generate sufficient data to test (5.9) for various camera distances, 6237 data points were generated for 11 camera distances ranging from 1-6ft, 9 heat generation values, 7 areas, and 9 flaw depths. All of the data was gathered in single run with a total computational time exceeding 100 hours. The same model, equation (5.9), was tested to see if it provided a reliable fit for each of the camera distances. It was found that for distances of 4 ft or less, equation (5.9) serves as a reasonable fit, however, as the camera distance increases, the R^2 value drops and the RMS error rises substantially. This behavior is seen in figures (5.7) and (5.8), where it is clear that

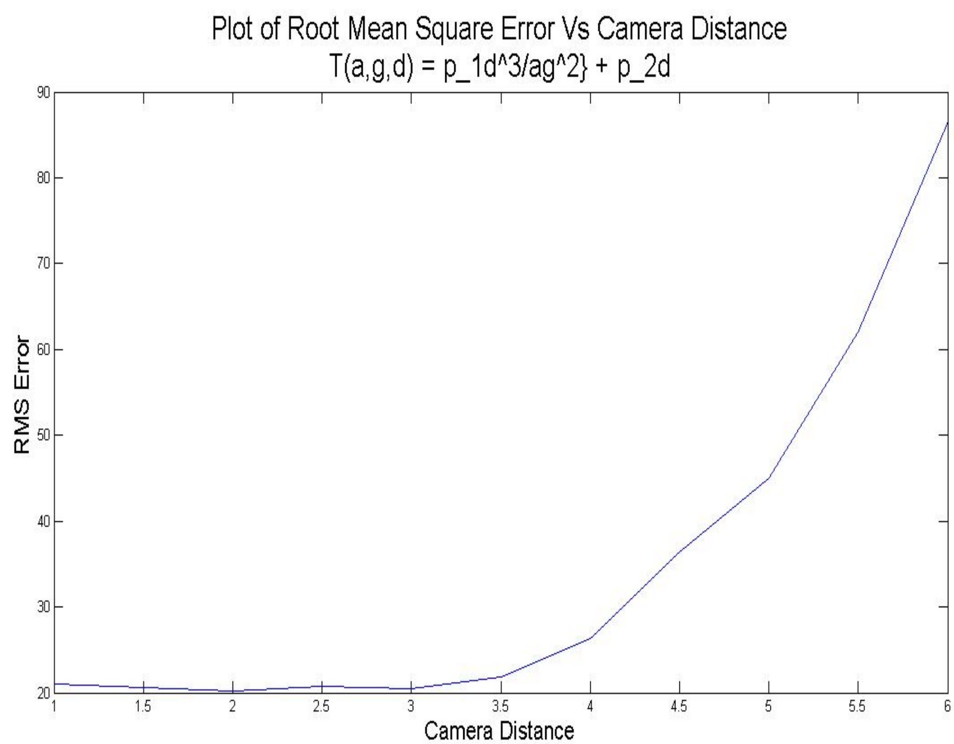

Figure 5.7: Variation of root mean square error with camera distance

the model accuracy diminishes rapidly with camera distances over 4 ft.

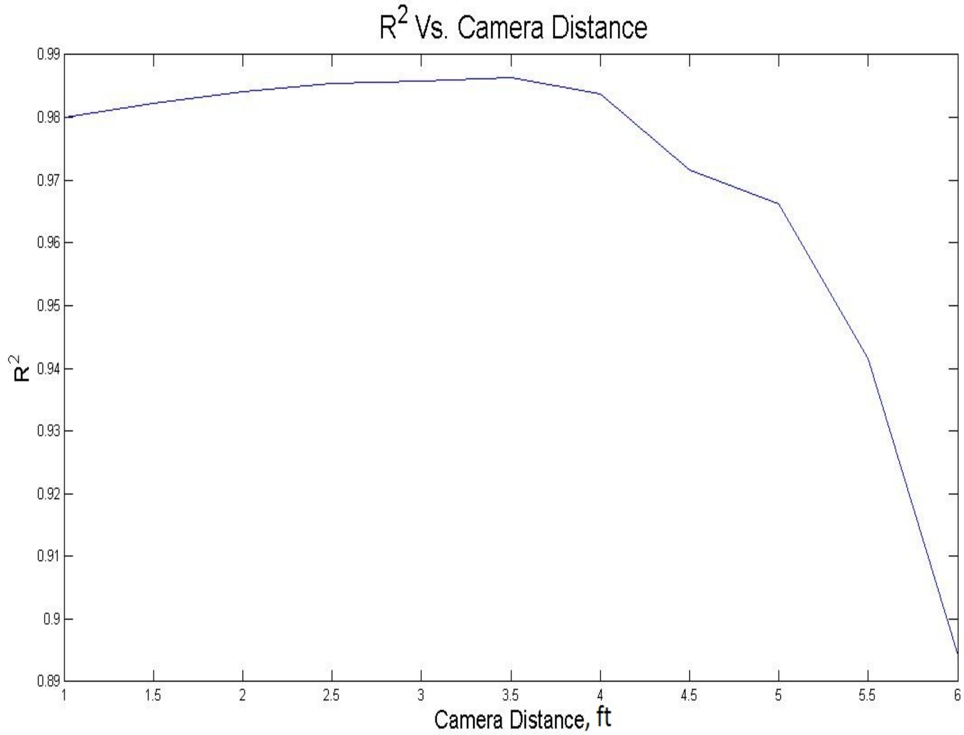

Figure 5.8: Goodness of fit according camera distances

Because each camera distance had an independent data set that was fit to (5.9), it is instructive to see how the free variables p_1 and p_2 varied with camera distance. A generally linear trend was observed for p_1 which can be seen in figure (5.9) The best linear fit for p_1 is also displayed in (5.9), and is given by the equation

$$p_1 = 1023.2d_c + 7424 \tag{5.10}$$

where d_c is camera distance in feet. This equation could be used for intermediate camera distances, however, the linear fit in (5.10) departs from the 95% confidence intervals for these values that were obtained in each surface fit. It would most likely be more accurate to perform a linear interpolation between data points, than to utilize (5.10).

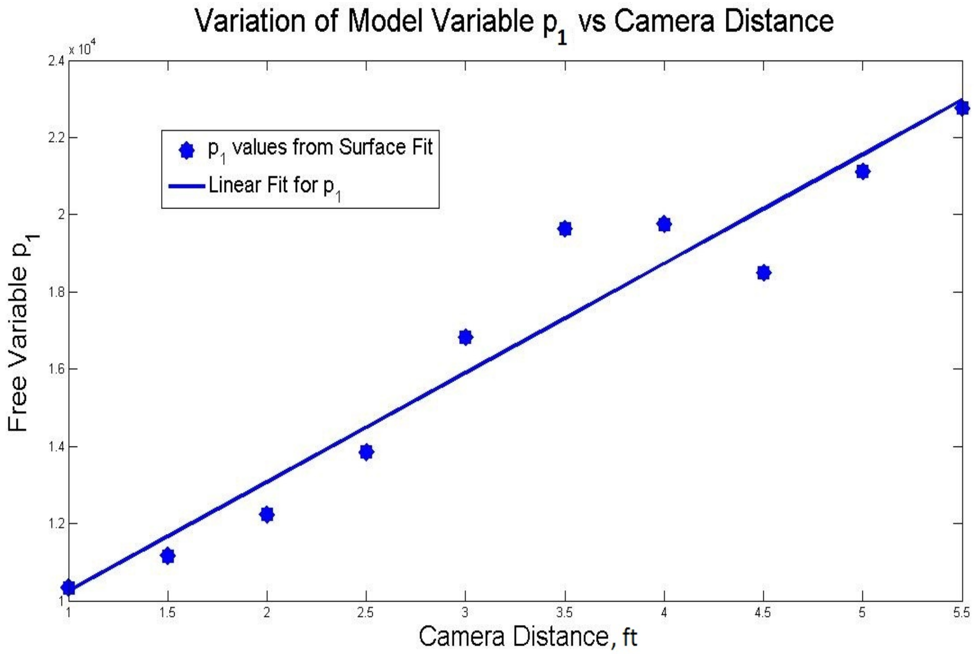

Figure 5.9: Variation of p_1 with camera distance

Limits of Detection

The FEA model used to generate detection times for various flaws also indicated which flaws were undetectable, creating clear boundaries on the limits of this NDT method in terms of flaw size, depth, and generation rate. A flaw is considered undetectable at a given camera distance if take over 30 minutes to produce the necessary surface temperature distribution that signals detection. The ANSYS output would provide a time value of -1 if the detection failed to occur for the steady state temperature distribution, and a value of -5 was assigned for those flaws that passed the steady state criterion, yet still failed to be detected after 30 minutes. This value of 30 minutes was selected both to limit the computation time of the simulations, and to match realistic expectations for how long a flaw might experience continuous excitation during a test. 1000 data points were gathered in a simulation that investigated the detectability and time until detection for plates of thicknesses up to 2" and flaws of depths up to 40.6mm. The results in terms of detectability are provided in table (5.1), where a $\surd$ marker indicates that all flaws ranging from $1/4 - 1in^2$ were detectable, an **X** marker indicates that no flaws were detectable, and a fraction indicates the smallest detectable flaw size. Only in a few instances was a flaw detectable at some camera distances and not others, so that information is omitted.

Table 5.1: Boundaries of Detection

	Heat Generation (W/m^2)				
Depth (mm)	12.5	50	125	250	500
1.27	3/4	$\surd$	$\surd$	$\surd$	$\surd$
2.54	1	$\surd$	$\surd$	$\surd$	$\surd$
3.81	1	$\surd$	$\surd$	$\surd$	$\surd$
4.23	**X**	$\surd$	$\surd$	$\surd$	$\surd$
5.08	**X**	$\surd$	$\surd$	$\surd$	$\surd$
7.20	**X**	1/2	$\surd$	$\surd$	$\surd$
8.46	**X**	1/2	$\surd$	$\surd$	$\surd$
10.16	**X**	1/2	$\surd$	$\surd$	$\surd$
12.70	**X**	3/4	$\surd$	$\surd$	$\surd$
14.40	**X**	3/4	1/4	$\surd$	$\surd$
16.93	**X**	3/4	1/4	$\surd$	$\surd$
20.32	**X**	**X**	3/4	$\surd$	$\surd$
21.59	**X**	**X**	3/4	$\surd$	$\surd$
28.79	**X**	**X**	1	1/2	$\surd$
30.48	**X**	**X**	**X**	3/4	1/2
40.64	**X**	**X**	**X**	**X**	3/4

Thermal Model Conclusions and Suggestions

The model provided by (5.9) provides a decent rule-of-thumb suggestion that could be used as a preliminary basis for a vibrothermographic heat detection algorithm; however, a more reliable method could be generated by creating at least one or more model to apply for longer detection times. Although it may appear that there is correlation between individual parameters such as camera distance and the accuracy of (5.9), the error[2] is most dependent on the detection times. The model is substantially more accurate for smaller detection times in terms of absolute error. Figure (5.10) provides a plot of the model accuracy vs detection times for over 500 data points corresponding to the camera distance of 3ft. The correlation between

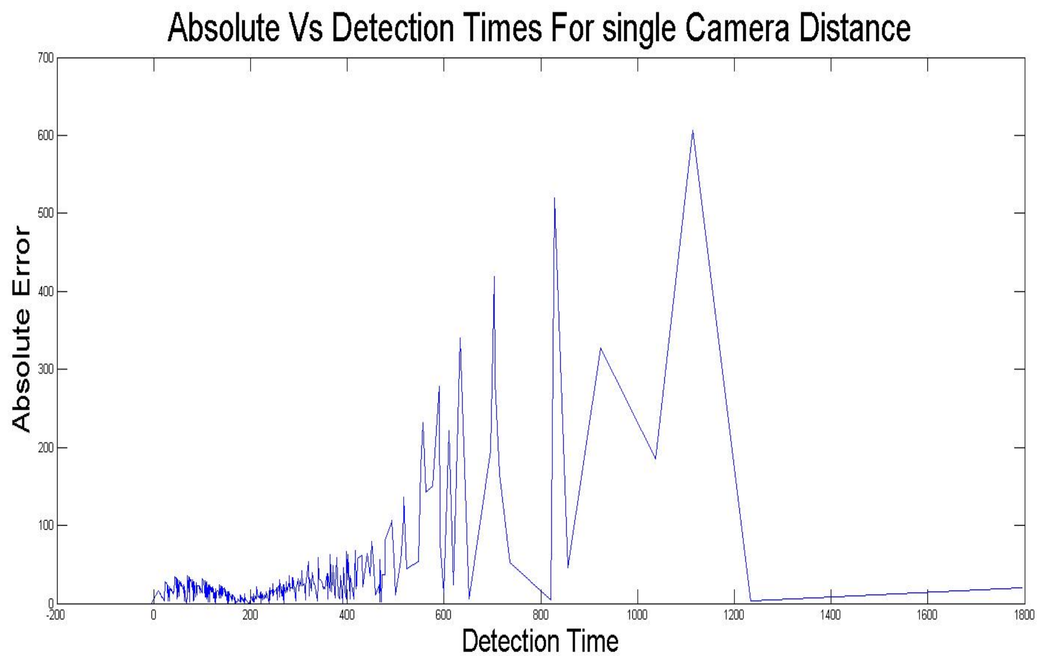

Figure 5.10: Absolute error of (5.9) plotted for detection times at an intermediate camera position.

model accuracy and detection times is clear from this plot. In particular, the error increases abruptly for those flaws with detection times over 600s, which comprises 17 of the 567 data points. Improvements could be made by creating separate models for detection times above and below 600s, so that each model was a better predictor of detection times for flaws in those respective time ranges.

[2]It should be noted that the *error* is quantified in terms of agreement between (5.9) and the FE results, and doesn't incorporate the error inherent in using FEA to determine detection times.

The error in (5.9) for large time can also be understood based on a temperature plot for particular point in the FEA model. Recall, that the model we have created is implicitly the model of the inverse temperature function. That is, if $T(t) = f(t)$, then we are trying to model the function $\Gamma = f^{-1}(T)$. For larger times, this function, f^{-1} becomes more poorly conditioned, meaning that small changes in the argument T lead to large changes in the resulting time $f^{-1}(T)$. This problem is illustrated in the figure (5.11) where the effects of temperature data error results in larger changes in

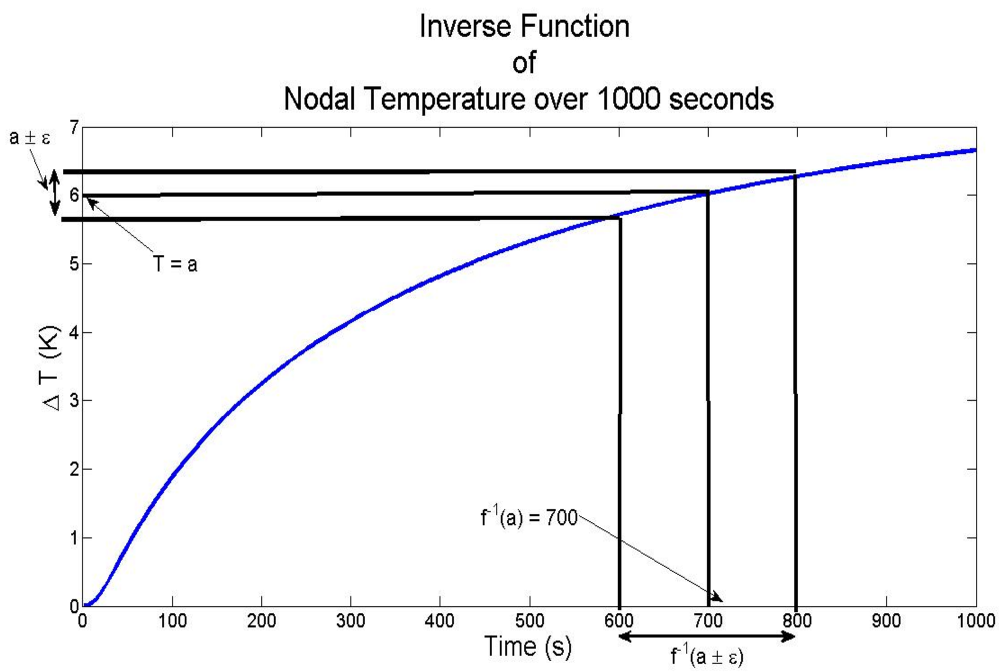

Figure 5.11: Poor conditioning of problem for large times.

detection times as a result of the temperature function asymptotically approaching steady state. It is clear that the problem becomes increasingly ill conditioned for larger times. This can also be understood by examining the derivative

$$\frac{d}{dT} f^{-1}(T) = \frac{1}{f'\left(f^{-1}(T)\right)} \tag{5.11}$$

The numerator in (5) is increasingly small as for larger values of T, which physically means that as time passes the material approaches steady state. In fact

$$\lim_{T \to T_\infty} \frac{d}{dT} f^{-1}(T) = \infty \tag{5.12}$$

where T_∞ is the steady value of the temperature at the point of interest. Now, when a flaw has a long detection time, the system is closer to steady state, and thus the problem conditioning gets worse. A large value for the derivative of f^{-1} means that small changes in the argument result in large changes in the output.

We can see this problem illustrated well by examining the confidence intervals for the parameters p_1 and p_2 in (5.9), described by $(p_1 - \epsilon_1, p_1 + \epsilon_1)$ and $(p_2 - \epsilon_2, p_2 + \epsilon_2)$ and how they affect the confidence interval for the detection time, $t - \Delta t/2, t + \Delta t/2)$, described by:

$$\Delta t = (p_1 + \epsilon_1)d^3/\zeta + (p_2 + \epsilon_2)d - (p_1 - \epsilon_1)d^3/\zeta + (p_2 - \epsilon_2)d = 2\epsilon_1 d^3/\zeta + 2\epsilon_2 d \tag{5.13}$$

Notice that as either d increases, or ζ decreases, the width of the confidence interval for detection time get increasingly broad. This is a natural result of the problem conditioning for large time, and will persist regardless of the model selected for larger times. It also interesting to note that the poor conditioning of the problem is directly related to diffusivity of the material. In the case of glass/epoxy composites, the low diffusivity means that the material will approach steady state more slowly, and problem is better conditioned than for a material like aluminum, where the fast conduction of heat results the derivative $\partial T/\partial t$ to rapidly vanish. Therefore, the accuracy of (5.9) for other materials should be given with respect to the product αt.

Regardless of the conditioning problem, there is still plenty of room to enhance the accuracy of the detection time model. As mentioned earlier, instead of pursuing a single model to encompass all detection times, it may be possible to devise separate models for large and small times. By dividing the data into two classes - say flaws for detection times above and below 500s, the two models could be used to provide a better fit for their respective data sets than the one model does. Another approach would be to generate data for a larger range of detectable flaw configurations and generation rates, so that an interpolating function, such as a spline interpolation could be used. This would require more work in determining the boundaries of detectability in terms of the flaw variables, but would provide more accurate detection time estimates for flaws within those bounds.

The purpose of determining a detection time model for various flaws is to aid in the development vibrothermographic detection routine for composite materials that optimizes the likelihood of detecting a flaw while minimizing the time required to test a large structure such as a wind turbine blade. By itself, the model developed in (5.9) is insufficient because it has yet to be determined whether heat generation at a flaw due to ultrasonic excitation can be parametrized or sufficiently predicted based on flaw size and depth. As seen in figures (3.3) and (4.9) the actual heat generated by a flaw can be very localized and seems to be determined by other factors such as boundary conditions and positioning relative to stress concentrations in harmonic waveforms. Nevertheless, if through FE modeling or experimental verification a reliable characterization of heat generation can be produced for vibrothermographic systems, then a model, such as (5.9), can be utilized to develop a detection routine.

CONCLUSIONS

Vibrothermography is a promising NDT method for finding delaminations in composite materials, but it's advancement has been hindered by the lack of development of a reliable testing scheme. Though it has has been clearly demonstrated that a cracked material may exhibit localized heating in the region of a flaw when vibrated at high frequencies, there is still no means of effectively controlling that heat generation or even ensuring that it will occur. One major problem is the current lack in understanding of the mechanics behind the heat generation. Even with the knowledge that the localized heating is due to fricional effects, there still is no accepted physical model to describe the surface interaction for these systems. Instead, an evergrowing body empirical data is the primary means of understanding these systems. In recent years, FEA has been used to simulate these systems, and could be the key to generating a reliable vibrothermographic model that may then be used to create an effective testing algorithm.

FE simulations have been able to match temperature results for a some vibrothermographic systems, but it remains to be demonstrated how effectively these methods can be used to *predict* such results for an arbitrary system. Without an accepted mathematical model of the flaw site frictional heat generation, the only means of verifying the FE simulations is through comparison to empirical data. Those comparisons are usually made in terms of maximum surface temperatures, since that is the only data available from physical tests. Chapter (4) presents one such FE model and examines how to more effectively employ FEA methods for these problems. It was found that the FE model was in reasonable agreement with the experimental values in terms of maximum surface temperatures after 180 seconds of exitation time. This means that FEA may be used to predict the steady state behavior of the vibrothermographic systems when long exitation times are necessary, as will be the case for the detection of fully embedded flaws. However, it remains to be demonstrated how variations in the flaw heat generation can affect these results, and whether it can be concluded the order-of-magnitude agreement of surface temperature data at a single point and at one time step implies agreement of heat generation rates between the model and physical system. Additionally, it was found that the presence of lower order modes during the transient mechanical response has a substantial effect on the rate of frictional heat generation, and that in order to produce steady state heat generation data, steady state mechanical response mush first be achieved. The resulting steady state heat generation rates are somehow proportional to the displacement amplitude, and thus damping parameters in the FE model need to be properly selected.

In addition to ensuring a proper mechanical response, it should also be verified that the surface interaction model adequately describes the system. When a penalty based contact algorithms is used, this means selecting contact stiffness constants that create a realistic state of stress at the flaw faces, and choosing frictional constants (usually for the Coulomb friction model) that, combined with the contact stresses, will result in frictional heat generation rates that match the system being modeled. Although it is not known how well penalty based contact and the Coulomb friction model describe the surface interaction of delamination faces during high frequency exitation, it has been shown that the heat generation results from these formulations produce temperature distributions that correlate well with empirical data.

The long computation times required to simulate these systems are a major hindrance towards effeciently generating data, however, the use of dynamic submodeling for large systems substantially expedites the process. By determining the steady state response along the boundary of a volume containing the delamination, a sub-model routine can apply those results as boundary conditions for the same volume but with a refined mesh around the delamination. This method drastically reduces the run-time of these simulations, however, it was found that even when using the sub-modeling method, the computation time required by the coarse model to reach steady state was prohibitively long when results are desired for a large frequency span. This problem can be overcome by utilizing the results from a harmonic analysis instead of a transient analysis, if it can be demonstrated that the presence of the delamination does not significantly effect the steady state response along the sub-model boundary. This is because a harmonic analysis in Ansys does not incorporate non-linearities such as contact.

If reliable heat generation values can be efficiently obtained using these methods, and if it's found that the potential frictional heat generation between flaw faces is predominantly characterized by flaw size, depth and area, then a detection model such as the one proposed in Chapter (5) can be used in the creation of a vibrothermographic detection routine. The model given in equation (5.9) correlates well with the flaw detection time values obtained using FE simulations of finite heat generating disks in a $1in$ composite plate, however, the model's accuracy is questionable for flaws with large detection time. This is due to the increasingly poor problem conditioning as the system approaches steady state, and possibly the inherent difficulties of finding a one-size-fits-all model. Unfortunately, the heat conduction problem associated with these systems can only be solved numerically, and so more work should be done to insure that the FEA solutions are *increasingly* accurate for large detection times. The FE simulation used to generate the data was optimized in terms of detection times for flaws of intermediate depths, sizes and generations. In order to improve the accuracy of (5.9) more reliable data could be produced by insuring that mesh refinements and time steps are chosen to better suit those flaws with long detection times, since they are inherently more sensitive to small temperature errors.

REFERENCES CITED

[1] Peter Lucon Kyle Kapp. Vibration induced temperature changes for verification of heat conduction/generation model. Technical Report, Resodyn Corporation, July 2011.

[2] Ahsan Mian, Golam Newaz, Xiaoyan Han, Tonfiz Mahmood, Chinmoy Saha. Response of sub-surface fatique damage under sonic load - a computational study. *Composites Science and Technology*, 64:1115–1122, 2004.

[3] E.G Heneke, K.L. Reifsnider, W.W. Stinchcomb. Vibrothermography: Investigation, development, and application of a new nondestructive evaluation technique. Technical Report, U.S. Army Research Office, 1986.

[4] Jeremy Renshaw, John C. Chen, Stephen D Holland, Bruce Thompson. The sources of heat generation in vibrothermography. *NDT and E International*, 44(8):736–739, December 2011.

[5] Jeremy Renshaw. *The Mechanics of Defect Detection in Vibrothermography*. Doctoral Dissertation, 2009.

[6] Stephen D Holland, Christopher Uhl, Jeremy Renshaw. Vibrothermographic crack heating: A function of vibration and crack size. *AIP Conference Procedings*, page 489, March 2009.

[7] Xiaoyan Han, Islam Md Sarwar, G Newaz, L.D Favro, R.L. Thomas. Finite element modeling of the heating of cracks during sonic infrared imaging. *Journal of Applied Physics*, 99, 2006.

[8] F Mabrouki, M Thomas, M Genest, A Fahr. Frictional heating model for efficient us of vibrothermography. *NDT and E International*, 42:345–352, July 2009.

[9] L Pieczonka, F. Aymerich, G. Brozek, M. Szwedo, W.J. Staszewski, T. Uhl. Modelling and numerical simulations of vibrothermography for impact damage detection in composites structures. *Structural Control and Health Moniter*, February 2012.

[10] R. Plum, T. Ummenhofer. Structural-thermal fe simulation of vibration and heat generation of cracked steel plates due to ultrasound excitation used for vibrothermography. *10th International Conference on Quantitative IfraRed Thermography*, July 2010.

[11] Ahsan Mian, Xiaoyan Han, Sarwar Islam, Golam Newaz. Fatigue damage detection in graphite/epoxy composites using sonic infrared imaging technique. *Composites Science and Technology*, 64:657–666, 2004.

[12] B.R. Vidyashanker, A.V. Krishna Murty. Analysis of laminates with ply drops. *Composites Science and Technology*, 61(5):749–758, April 2001.

[13] Joakim Schön. Coefficient of friction of composite delamination surfaces. Technical Report, The Aeronautical Research Institute of Sweden, Bromma, Sweden, September 1999.